Journal of Cleaner Production 360 (2022) 131750

Contents lists available at ScienceDirect

Journal of Cleaner Production

journal homepage: www.elsevier.com/locate/jclepro

A climate-optimal supply chain for CO_2 capture, utilization, and storage by mineralization

Hesam Ostovari [a], Leonard Müller [a], Fabian Mayer [a,c], André Bardow [a,b,c,*]

[a] Institute of Technical Thermodynamics, RWTH Aachen University, Germany
[b] Institute of Energy and Climate Research - Energy Systems Engineering (IEK-10), Forschungszentrum Jülich GmbH, Jülich, Germany
[c] Energy & Process Systems Engineering, ETH, Zurich, Switzerland

ARTICLE INFO

Handling Editor: Yutao Wang

Keywords:
Carbon capture and utilization
Mineralization
Carbonation
Supply chain optimization
Negative emission
Greenhouse gas mitigation

ABSTRACT

CO_2 mineralization not only captures and stores CO_2 permanently but also yields value-added products utilized in, for example, the cement industry. CO_2 mineralization has been shown to potentially substantially reduce greenhouse gas (GHG) emissions. Realizing CO_2 mineralization's potential on a large scale requires *a) solid feedstock, b) CO_2 sources, c) low-carbon energy,* and *d) markets for mineralization products.* In general, these four requirements of CO_2 mineralization are not satisfied at the same location. Thus, the assessment of CO_2 mineralization's large-scale potential necessitates the full supply chain considering all requirements for CO_2 mineralization simultaneously. At present, neither the potential of CO_2 mineralization for GHG emissions reduction on a large scale nor the required supply chain to achieve the potential are fully understood. In our study, we design a climate-optimal supply chain for CO_2 capture, utilization, and storage (CCUS) by CO_2 mineralization to quantify the large-scale potential of CO_2 mineralization in Europe. Our results show that a climate-optimal CCUS by CO_2 mineralization could avoid up to 130 Mt CO_{2e}/year of the industrial emissions in Europe even with the current energy supply system. By 2040, CCUS by CO_2 mineralization could provide negative emissions of up to 136 Mt CO_{2e}/year. The required energy and CO_2 for the CCUS supply chain can be provided either by expanding the current infrastructure by about 5 % or, even more climate efficiently, by building new infrastructure. The critical steps toward achieving the large potential of CO_2 mineralization in Europe are 1) scaling up the CO_2 mineralization technology to the industrial level and 2) exploiting large-scale mineral deposits.

1. Introduction

The industry sector emits around 8 Gt CO_{2e} per year, contributing 23 % of global greenhouse gas (GHG) emissions (IEA, 2019). The GHG emissions of the industry sector could be reduced by substituting fossil energy with renewable energy. However, energy substitution is not sufficient, as part of the industry sector's GHG emissions is process-inherent since CO_2 is produced as a byproduct. This part of the industry sector's GHG emissions is particularly difficult to eliminate (Davis et al., 2018).

GHG emissions of the industry sector can substantially reduce by capture and storage of locally emitted CO_2 via carbon capture, utilization, and storage (CCUS) technologies (IEA, 2019). Two main approaches can permanently store the captured CO_2: geological storage and CO_2 mineralization. For geological storage, CO_2 is injected underground to be permanently stored (Bui et al., 2018). Several studies and pilot projects have investigated the GHG emissions mitigation potential of geological storage (Bui et al., 2018).

A less explored CO_2 capture and storage approach is CO_2 mineralization (Romanov et al., 2015). In CO_2 mineralization, CO_2 reacts with calcium oxide- (CaO) or magnesium oxide- (MgO) bearing materials to produce stable carbonates that can store CO_2 for millions of years (Lackner, 2003). Equations (1) to (3) show CO_2 mineralization of three MgO/CaO bearing materials: forsterite (the main component of olivine), serpentine, and calcium silicate (the active component of steel slag), respectively (Bremen et al., 2021; Chen et al., 2006; Huijgen et al., 2006).

$$Mg_2SiO_4 + 2\ CO_2 \rightarrow 2\ MgCO_3 + SiO_2 + \text{heat} \quad (1)$$

$$Mg_3Si_2O_5(OH)_4 + 3\ CO_2 \rightarrow 3\ MgCO_3 + 2\ SiO_2 + 2\ H_2O + \text{heat} \quad (2)$$

$$Ca_2SiO_4 + 2\ CO_2 \rightarrow 2\ CaCO_3 + SiO_2 + \text{heat} \quad (3)$$

---

* Corresponding author. Energy & Process Systems Engineering, ETH Zurich, Switzerland.
E-mail address: abardow@ethz.ch (A. Bardow).

https://doi.org/10.1016/j.jclepro.2022.131750
Received 4 November 2021; Received in revised form 29 March 2022; Accepted 11 April 2022

Besides capturing and permanently storing CO_2, mineralization yields products that can be utilized. A promising pathway is the utilization of SiO_2 in the cement industry to partially substitute clinker (Benhelal et al., 2018, 2020). Clinker substitution increases the environmental benefits of CO_2 mineralization (Woodall et al., 2019). Although CO_2 mineralization is thermodynamically favorable, several energy-intensive processes are required to overcome its slow reaction kinetics. The emissions arising from the required energy-intensive processes could offset the potential of mineralization to reduce GHG emissions. Yet, several studies have shown that, under favorable conditions, CO_2 mineralization technology has a large potential to reduce GHG emissions by CO_2 storage and utilization (Chiang and Pan, 2017; Gerdemann et al., 2007; Giannoulakis et al., 2014; Ostovari et al., 2020; Pan et al., 2016; Woodall et al., 2019).

Several studies investigated solid feedstocks' availability to estimate the potential of CO_2 mineralization on a large scale. Worldwide, natural mineral feedstock available for CO_2 mineralization is estimated as 10^8 Gt, which is sufficient to mineralize $5 \cdot 10^7$ Gt CO_2 (Bide et al., 2014; Bodénan et al., 2014; Hovorka and Kelemen, 2021; Julcour et al., 2015; Kirchofer et al., 2013; Kremer et al., 2019; Lackner et al., 1995; Pedro et al., 2020; Picot et al., 2011; Power et al., 2013; Renforth, 2019; Sanna et al., 2014; The National Academies Press, 2019). This potential is seven orders of magnitude larger than the annual global CO_2 emissions of above 40 Gt CO_2 (IPCC, 2018). However, none of the studies mentioned above considered the emissions arising from the required energy-intensive processes for CO_2 capture, CO_2 mineralization, or transport.

Recently, Pan et al. (2020) estimated the large-scale potential of industrial byproduct mineralization for GHG emissions reduction. According to Pan et al.'s results, mineralization could directly reduce 54.4 Mt CO_2 emissions per year in Europe. This estimation corresponds to an upper bound since the analysis did not consider emissions from solid feedstock transport, CO_2 transport, CO_2 capture, or the CO_2 mineralization process. By assuming an unlimited cement market size, Pan et al. estimated an additional indirect CO_2 reduction of 860 Mt CO_{2e} emissions per year in Europe via cement substitution (Pan et al., 2020). Notably, the emissions reduction of 860 Mt CO_{2e} per year cannot be achieved by the current cement production rate in Europe since the CO_2 emission from the cement sector in Europe is below 150 Mt CO_{2e} per year (European Environment Agency, 2019).

Realization of the large-scale potential of CO_2 mineralization requires not only *a) solid feedstock, b) markets for mineralization products,* but also *c) CO_2 sources, d) low-carbon energy (Ostovari et al., 2021)*. In particular, solid feedstock, the markets for mineralization products, CO_2 sources, and low-emission energy are normally not available at the same location. Consequently, either CO_2 must be transported to the solid feedstock, or solid feedstock must be transported to locations with available CO_2 and product market. Emissions arising from energy demand of mineralization on the one hand and transport of CO_2, solid feedstock, or products, on the other hand, limit the large-scale potential of CO_2 mineralization to reduce GHG emissions. Furthermore, the capacity of the cement market to utilize the byproducts of mineralization is limited. Thus, the large-scale potential of CO_2 mineralization for GHG emissions reduction is currently not fully understood.

To estimate the large-scale potential of CO_2 mineralization, the full supply chain for CO_2 mineralization needs to be designed. However, the design is not straightforward as the following parameters need to be considered simultaneously:

a) *location and amount of available solid feedstock which can be extracted for CO_2 mineralization,*
b) *demand for utilizing the mineralization products,*
c) *location and amount of available CO_2 sources which can be equipped with CO_2 capture,*
d) *Network required for CO_2 transport,*
e) *carbon footprint of energy supply along the supply chain* (Hasan et al., 2014, 2015; The National Academies Press, 2019).

Several studies investigated the potential of a supply chain for CO_2 capture, transport, and geological storage in Europe (d'Amore et al., 2021; d'Amore et al., 2019; d'Amore and Bezzo, 2017; Elahi et al., 2014; Gabrielli et al., 2020). More recently, researchers have extended the supply chain to include CO_2 utilization; however, none of the studies mentioned above have considered CO_2 mineralization as a potential technology of carbon capture, utilization, and storage (d'Amore and Bezzo, 2020; Leonzio et al., 2020; Zhang et al., 2020). Recent studies focused on multi-objective optimization of process parameters for a variety of CCUS technologies that could be integrated into CCUS supply chains (Fazlinezhad et al., 2022; Hazrati-Kalbibaki et al., 2020). Common CCUS supply chains match CO_2 sources to CO_2 sinks with fixed location (d'Amore and Bezzo, 2020; Kalyanarengan Kalyanarengan Ravi et al., 2017; Morbee et al., 2012). However, CO_2 sink locations are degrees of freedom in a CCUS by mineralization supply chain. Even more, the supply chain needs to provide the CO_2 sinks with suitable solid feedstock while considering the possible utilization or storage of the mineralization products as well as the penalty of the regional energy system. These aspects increase the complexity of supply chain optimization for CCUS by mineralization. Thus, at present, neither the potential of CO_2 mineralization for GHG emissions reduction on a large scale nor the required supply chain to achieve the potential are fully understood.

In this paper, we quantify the potential for large-scale GHG emissions reduction of CO_2 mineralization by designing a climate-optimal supply chain for CO_2 capture, utilization, and storage by mineralization in Europe, including emissions rising from the entire life cycle of CO_2 capture, CO_2 mineralization, and transport.

Section 2 presents the data considered along the entire CCUS by CO_2 mineralization supply chain. In section 3, we introduce our matching approach for a climate-optimal CCUS supply chain. Our base-case scenario in section 4.1 presents the GHG emissions mitigation potential of CCUS by mineralization supply chain on a large scale. Section 4.2 analyzes the supply chain of the CCUS by mineralization via five scenarios for CO_2 supply, energy supply, and solid feedstock availability. In section 5, we conclude our results and derive an outlook for the supply chain of CCUS by mineralization.

2. Technologies, scope, and data for the CO_2 mineralization supply chain

To identify the climate-optimal supply chain for CO_2 mineralization, we need data for *a) solid feedstock sources (Section 2.1), b) CO_2 feedstock sources (Section 2.2), c) energy supply (Section 2.3)*, and *d) CO_2 capture, utilization, and storage by mineralization (Section 2.4)*. In the following sections, we present our considered data and the scope (Section 2.5) for the entire CCUS by mineralization supply chain.

2.1. Solid feedstock sources

Solid feedstock for CO_2 mineralization can be obtained from natural minerals or industrial wastes with a high portion of calcium oxide (CaO) or magnesium oxide (MgO), e.g., ultramafic rocks, or electric-arc furnace steel slag (Romanov et al., 2015).

Currently, five commercial mines are mining olivine or serpentine (natural minerals) in Europe (Fig. 1). The five active mines in Europe produce more than half of the global olivine production and could

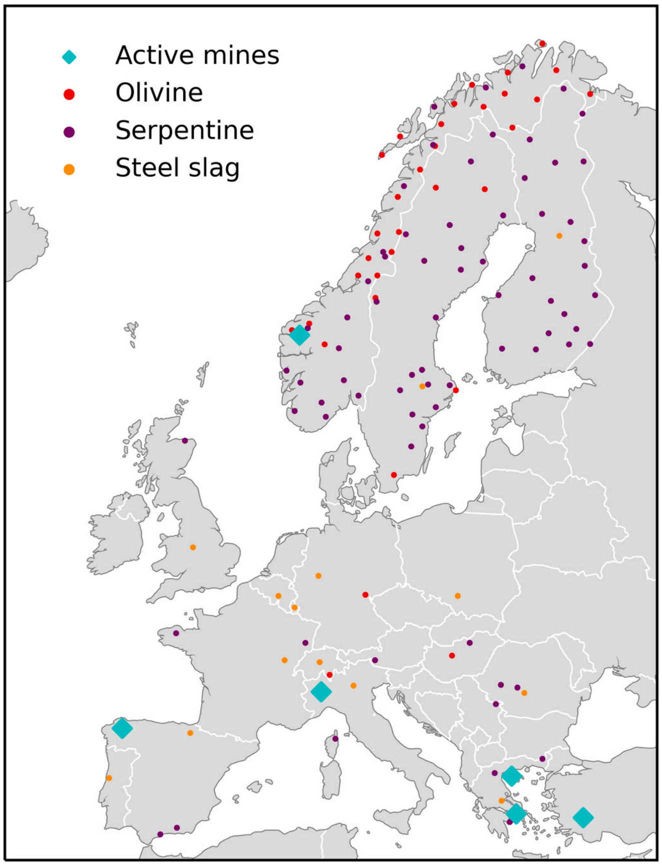

Fig. 1. Distribution of solid feedstock for CO_2 mineralization in Europe including: currently active mines of natural minerals, potential locations of natural minerals (olivine and serpentine), and locations of steel slag from electric arc furnace (EAF) steel production.

supply the solid feedstock of mineralization (Kremer et al., 2019). In addition to the existing mines, potentially about 107 locations in Europe could be explored for mining of natural minerals (mafic, ultramafic) compatible for CO_2 mineralization (Fig. 1 and ESI Section S5) (Bide et al., 2014; Bodénan et al., 2014; Hudson Institute of Mineralogy dba; Julcour et al., 2015; Minerals4EU database; Picot et al., 2011; ProMine database; Veld et al., 2009).

For industrial wastes, we consider 14 locations for steel slag from electric-arc furnaces in Europe (EUROFER database). The production capacity of each plant is low, and plants within one country are in close range of each other. Therefore, we simplify our model by aggregating the entire amount of steel slag produced per country in the geological center of all national production sites (Fig. 1). Steel slag from blast furnaces is already utilized in the cement industry (World Steel Association, 2018a); therefore, we do not consider steel slag from blast furnaces as a solid feedstock of CO_2 mineralization.

We assume that the maximum transport distance of solid feedstock is 500 km as a typical maximum distance for transport of cement or cheap bulk materials (EUROPEAN COMMISSION, 2018). Therefore, mineralization plants can be located either exactly at the location of a solid feedstock or in a radius of 500 km (see ESI Section S5).

Other promising locations to mine solid feedstock exist outside Europe, e.g., in Australia, Oman, South Africa, and North America. Due to long-distance transport and infrastructural barriers (Hangx and Spiers, 2009), we do not consider the possibility of importing solid feedstock from other continents in our study.

Besides the solid feedstock location, its extraction capacity needs to be known for the CCUS supply chain. For the *base-case scenario,* we assume that the maximum extraction capacity of a natural mineral (olivine or serpentine) mine is 10 Mt minerals/year. The extraction capacity of a mine highly depends on its mineral deposit. 10 Mt minerals/year is chosen as the medium size of copper open-pit mines in Europe. Noteworthy, a copper open-pit mine can reach up to 40 Mt ores/year, e.g., Aitik copper mine in Sweden (Hustrulid and Kuchta, 2006; New Boliden). The current extraction capacities of the five active mines are much lower than the 10 Mt minerals/year (see ESI Section S5). Yet, if the market for natural minerals grows, the mine's assumed extraction capacity for our *base-case scenario* can be theoretically achieved (Hustrulid and Kuchta, 2006; New Boliden). We discuss the effect of the extraction capacity on the CCUS supply chain in Section 4.2 and the ESI Section S2. For the maximum production capacity of steel slag from electric arc furnaces, we use the database of the World Steel Association (World Steel Association, 2018b).

2.2. *CO_2 feedstock sources*

In our study, we focus on the difficult-to-eliminate CO_2 sources from the industry sector; however, our model can be expanded to all kinds of CO_2 sources (see ESI Section S1 and S4). We consider the location and CO_2 amount of potential CO_2 point sources in Europe, according to von der Assen et al. (2016) and the report of the European Environment Agency (2019) (Fig. 2). Cement, steel, paper, and chemical industries directly emitted about 538 Mt CO_2 from 700 sites in 2017 (European Environment Agency, 2019). In our study, we refer to the GHG emissions from the cement, steel, paper, and chemical industries as the industry sector's GHG emissions. The fossil-fuel-based energy sector emitted about 965 Mt CO_2 from 800 sites in 2017 (European Environment Agency, 2019).

Transforming the energy sector towards renewable energy could

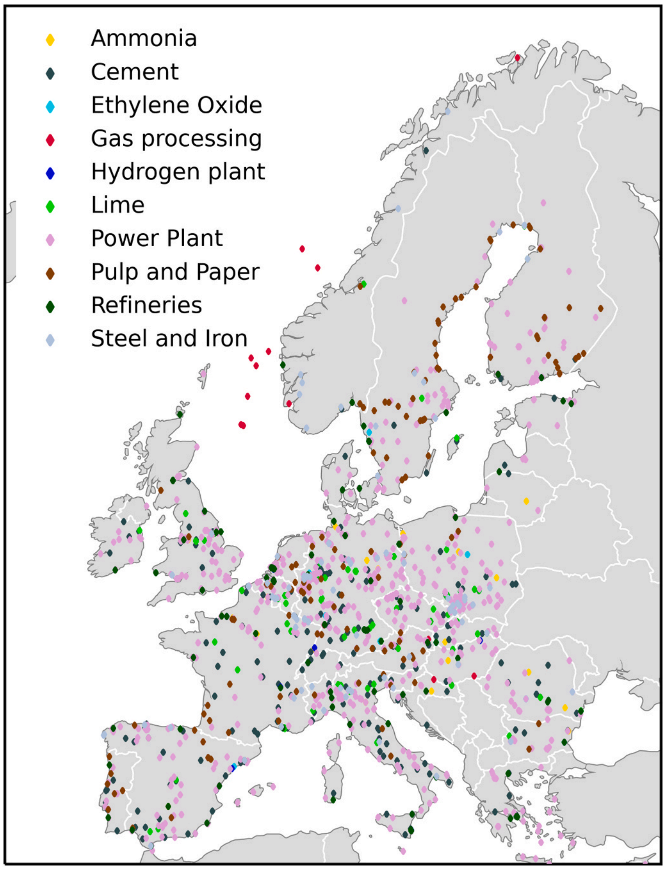

Fig. 2. Distribution of CO_2 sources from cement, steel, paper, and chemical industries in Europe (European Environment Agency, 2019; von der Assen et al., 2016).

theoretically reduce the direct emissions from the fossil-fuel-based energy sector to zero. To avoid blocking the technology transition in the energy sector (carbon lock-in effect, Mattauch et al., 2015; Seto et al., 2016), we do not consider CO_2 point sources of the energy sector in our main study. Nonetheless, as an alternative scenario, we design a CCUS supply chain capturing CO_2 from both industry and fossil-fuel-based energy CO_2 point sources (see *total CO_2 source scenario* in ESI Section S1).

The supply chain of CCUS by mineralization is not limited to CO_2 point sources. The required CO_2 for CCUS by mineralization can also be captured directly from the air via Direct Air Capture (DAC) plants. To illustrate this option, we define the *carbon-negative scenario* (see ESI Section S1 and S6). Capturing CO_2 from the atmosphere and permanently storing the captured CO_2 by mineralization could lead to negative emissions (Müller et al., 2020; Tanzer and Ramírez, 2019).

2.3. Energy supply

For the environmental impacts of thermal energy and electricity supply in each country, we use the most up-to-date LCA databases based on 2017 reports (GaBi 9.2. Software-System and Database for Life Cycle Engineering, 2019; Swiss Centre for Life Cycle Inventories, 2020). In our study, the thermal heat demand is assumed to be supplied by electric heating in locations where the carbon footprint of electricity is lower than of natural gas combustion; elsewhere, the required thermal heat demand is assumed to be supplied by natural gas.

In our *base-case scenario*, we consider the current electricity grid mix for each country. Assuming the European electricity grid mix could marginally lower the GHG mitigation potential of the CCUS supply chain (see ESI Section S1).

2.4. CO_2 capture, utilization, and storage (CCUS) by mineralization

Our study uses Life Cycle Inventory (LCI) data for CO_2 mineralization technologies, products utilization, cement industry, CO_2 capture, CO_2 pipeline, Direct Air Capture (DAC), solid feedstock mining, and transport from literature and LCA databases (see ESI Section S3).

We consider specific mineralization technologies depending on the solid feedstock (serpentine, olivine, and steel slag, see ESI Section S3, Figs. S17–S19, Kremer and Wotruba, 2020; Ostovari et al., 2020). Furthermore, to calculate the large-scale potential of CCUS by mineralization supply chain, we assume that the laboratory scale performances of CO_2 mineralization represent the future industrial-scale plant (Tanzer et al., 2020).

CO_2 mineralization produces carbonates ($CaCO_3$/$MgCO_3$) as the main product and silicate (SiO_2) as the byproduct. The locations and market sizes for the CO_2 mineralization byproduct (SiO_2) are based on cement plants' site and production capacity in Europe (European Environment Agency, 2019). As SiO_2, the byproduct of CO_2 mineralization, is not a self-cementing material, SiO_2 cannot entirely substitute cement. In our study, we consider 20 wt% cement substitution. Substituting 20 wt% of clinker in cement with SiO_2 has been shown to have a limited effect on the cement's performance (AlArab et al., 2020; Garrett et al., 2020; Ince et al., 2020).

The carbonates, the main product of CO_2 mineralization, could also be utilized in industry (Woodall et al., 2019). Yet, either the market size or the avoided GHG emissions for carbonates are limited (Sanna et al., 2012). Therefore, we do not consider the utilization of carbonates in our study. We assume that the carbonates are transferred back to the solid feedstock mine to be stored permanently.

For CO_2 point sources, the CO_2 capture technology in our study is state-of-the-art amine scrubbing. The energy demand of CO_2 capture differs based on the type of CO_2 source (see ESI Section S3 and Table S4). We design the CO_2 pipeline based on ASTM A53/A53M (2012) and the study of Wildbolz (2007). The energy demand of direct air capture is calculated according to Deutz and Bardow (2021).

We assume open-pit mining for the natural solid feedstock (Hangx and Spiers, 2009). The solid feedstock and the products are transported by trucks. We present all considered Life Cycle Inventory (LCI) data in ESI Section S3.

2.5. Goal and scope of the study

The goal of our study is to quantify the GHG emission mitigation potential of CCUS by mineralization and to assess the corresponding supply chain. For this purpose, we use the standardized method of life cycle assessment (LCA, ISO 14040:2021; ISO 14044:2021; ISO 14067:2018; ISO/TR 14049:2012) to calculate the avoided CO_{2e} emissions per year via CCUS by mineralization. LCA is regarded as the most systematic and holistic method to assess the environmental impacts of products or services by considering the entire life cycle (ILCD Handbook, 2010). By also considering several environmental impact categories, LCA identified potential problem shifting (ILCD Handbook, 2010). We determine the climate impact according to IPCC following the recommendation for LCA of the European Commission (ILCD Handbook, 2010). Other environmental impacts are determined with the ReCiPe life cycle impact method (Huijbregts et al., 2017). The results are presented for all impact categories in Section 4.3.

Due to the best data availability, we select Europe as the regional scope for our study. Noteworthy, our method can also be implemented in other regions of the world. We calculate the environmental impacts of required products or services for the CCUS by mineralization supply chain from cradle-to-grave (ESI Section S3).

For utilization of the products of the mineralization plants, we assume that the byproduct of mineralization SiO_2 is used in blended cement with 20 wt% (CEMII) and that this blended cement performs like conventional cement (CEMI) (AlArab et al., 2020; Deutsches Institut für Normung; Garrett et al., 2020; Ince et al., 2020). The main product of CO_2 mineralization, carbonates ($CaCO_3$/$MgCO_3$), store the CO_2 permanently and thus, could lead to CO_2 sink.

Our study analyzes the GHG emissions avoided by introducing CCUS by mineralization in the industry sector. For this purpose, we subtract the GHG emissions of the industry sector from those of the industry sector with an integrated CCUS by mineralization; the difference is the GHG emission mitigation of CCUS by mineralization (ILCD Handbook, 2010). All byproducts are identical in the industry sector with and without CCUS and thus cancel in the difference.

3. Matching approach for climate-optimal CCUS supply chain

A climate-optimal CCUS by mineralization supply chain avoids the most GHG emissions while fulfilling all the design constraints. Designing an optimal supply chain while considering all possible direct and indirect connections for the 1067 locations of CO_2 sink and 1500 locations of CO_2 sources in a single-stage optimization problem substantially increases the optimization problem size and, consequently, the required computational time. Previous work has shown that the exact configuration of the CO_2 pipeline network has a small contribution to the total GHG emissions of a CCUS supply chain (Middleton and Bielicki, 2009). Thus, we assumed that the impact of solving a two-step problem is small on the resulting solution quality. Following work on CCS supply chains, we design a climate-optimal CCUS by mineralization supply chain by solving a two-stage optimization problem to reduce the problem size and resulting computational time (Middleton et al., 2020; Middleton and

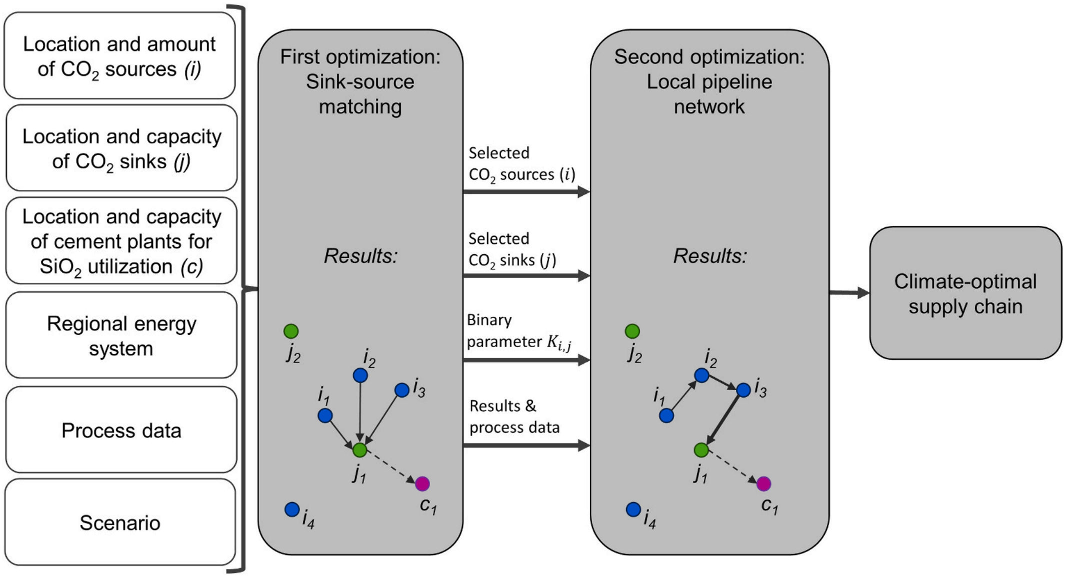

Fig. 3. Illustration of the sink-source matching and the local pipeline network optimization problems and their solutions. (*i*) indicates CO_2 sources. (*j*) marks possible locations for CO_2 sink. At cement plants (*c*), the byproducts of CO_2 mineralization can partially substitute cement.

Bielicki, 2009; Zhou et al., 2014). The first optimization problem (sink-source matching, Section 3.1) matches individually the CO_2 sources (*i*) to the CO_2 sinks (*j*) to maximize the amount of GHG emissions avoided due to CO_2 uptake and cement substitution while accounting for the indirect emissions due to transport, energy, and materials (Fig. 3). The matched pairs of CO_2 source and CO_2 sink are transferred to the second optimization problem: local pipeline network (Section 3.2). The local pipeline network optimization minimizes GHG emissions due to building and operating the required CO_2 pipeline network by merging CO_2 pipes into larger-sized pipes, thus, redesigning the local CO_2 pipeline network (Fig. 3).

3.1. *First optimization problem: sink-source matching*

Two mechanisms drive the GHG emissions mitigation of a CCUS by mineralization supply chain a) capturing and permanently storing CO_2 and b) substituting clinker by CO_2 mineralization byproduct. The clinker substitution reduces the clinker intensity of cement, thus reduces the cement industry's GHG emissions (Habert et al., 2020; Ostovari et al., 2021). For our sink-source matching problem, we modify the model of Hasan et al. (see Eq. 4, Table 1, and Hasan et al., 2014, 2015). The mixed-integer linear program (MILP) optimization model of Hasan et al. designs an economically optimal carbon capture and geological storage (CCGS) supply chain (Hasan et al., 2014, 2015).

In contrast to the economic problem, the objective function of our sink-source matching problem maximizes GHG emission mitigation via the CCUS by mineralization supply chain.

Objective Function:

Table 1
List of all variables and parameters of the sink-source matching optimization.

Variables	Parameters
$W_{c,j}, Y_{i,j},\ Z_j, Mass_j^{ExcessSiO2}$	$GHG_{i,j}^{avoidedbyCCS},\ GHG_{c,j}^{avoidedbyCCU},\ D_j^{ToStorage},$ $GHG^{SolidTransport},\ GHG^{SiteConstruction},\ F_i,$ $Size_j^{Max},\ Size_j^{Min},\ D^{LongestCO2},\ Mass_{i,j}^{ProducedSiO2},$ $Mass_{c,j}^{UtilizedSiO2}, D^{LongestSiO2},\ GHG_i^{capture},$ $\overline{GHG}_{i,j}^{CO2Transport}, GHG_{i,j}^{mineralization}, GHG^{AvoidedbySub}$ $GHG_{i,j}^{CarbonateTransport},\ GHG_{i,j}^{FeedstockTransport}, GHG_{i,j}^{mining}$ $GHG^{Cementproduction}, D_{c,j},\ Mass_c^{Cement}$

$$\begin{aligned}\max_{W_{c,j},Y_{i,j},\ Z_j,Mass_j^{ExcessSiO2}} & \sum_{i\varepsilon I}\sum_{j\varepsilon J}\left(GHG_{i,j}^{avoidedbyCCS}\cdot Y_{i,j}\right) \\ & +\sum_{c\varepsilon C}\sum_{j\varepsilon J}\left(GHG_{c,j}^{avoidedbyCCU}\cdot W_{c,j}\right) \\ & -\sum_{j\varepsilon J}\left(GHG^{SolidTransport}\cdot D_j^{ToStorage}\cdot Mass_j^{ExcessSiO2}\right) \\ & -\sum_{j\varepsilon J}\left(GHG^{SiteConstruction}\cdot Z_j\right),\end{aligned} \tag{4}$$

where *i* is a CO_2 source, e.g., cement plant, or steel plant, etc., *c* is a cement plant, and *j* is a CO_2 sink, i.e., a potential location for CO_2 mineralization plant (cf. section 2.1). Each solid feedstock source can supply only one mineralization plant in a radius of 500 km (see ESI Section S5). $c \in C$ is a subdomain of *I* that is including only the cement plants ($c \in C \subseteqq I$).

The objective function of our sink-source matching optimization consists of four parts:

i) *Carbon capture and storage.* $GHG_{i,j}^{avoidedbyCCS}$ is the amount of GHG emissions avoided if CO_2 from CO_2 source *i* is supplied to CO_2 sink *j*. The $GHG_{i,j}^{avoidedbyCCS}$ includes permanent storage of CO_2 from source *i* and emissions due to CO_2 capture, CO_2 transport, CO_2 mineralization, feedstock supply, feedstock transport, and transport of carbonates ($CaCO_3/MgCO_3$) to storage:

$$\begin{aligned}GHG_{i,j}^{avoidedbyCCS} \\ &= F_i - GHG_i^{capture} \\ &-\overline{GHG}_{i,j}^{CO2Transport} - GHG_{i,j}^{mineralization} \\ &-GHG_{i,j}^{mining} - GHG_{i,j}^{CarbonateTransport} - GHG_{i,j}^{FeedstockTransport}.\end{aligned} \tag{5}$$

Here, F_i is the amount of CO_2 captured from CO_2 source *i*, $GHG_i^{capture}$ quantifies the GHG emissions due to capturing CO_2 from the CO_2 source *i*, $\overline{GHG}_{i,j}^{CO2Transport}$ presents the GHG emissions caused by transporting CO_2 from the CO_2 source *i* to the CO_2 sink *j* via an individual direct pipe, assuming a diameter of 150 mm (Wildbolz, 2007). We refine the emissions of CO_2 transport in the local pipeline network optimization (cf. Section 3.2). $GHG_{i,j}^{mineralization}$ is the GHG emissions due to mineralizing CO_2 from CO_2 source *i* in mineralization plant *j*. $GHG_{i,j}^{mining}$ quantifies the

GHG emissions emitted by mining to mineralize CO_2 from CO_2 source *i* in mineralization plant *j*. $GHG^{CarbonateTransport}_{i,j}$ accounts for the GHG emissions due to transporting the carbonates produced by mineralizing CO_2 from CO_2 source *i* in mineralization plant *j* to the mine for backfilling. $GHG^{FeedstockTransport}_{i,j}$ are the GHG emissions caused by transporting the required feedstock to mineralizing CO_2 from the CO_2 source *i* in the CO_2 sink *j* (see ESI Section S3). The variable $Y_{i,j} \in [0,1]$ in the objective function indicates whether and to what extent CO_2 source *i* supplies CO_2 sink *j*.

ii) *Utilization of the product.* $GHG^{avoidedbyCCU}_{c,j}$ is the amount of GHG emissions avoided, if we utilize the produced silica (SiO_2) in mineralization plant *j* to substitute 20 wt% of clinker at cement plant *c* (Woodall et al., 2019). $GHG^{avoidedbyCCU}_{c,j}$ includes the avoided GHG emissions due to clinker reduction but also accounts for emissions due to transport of SiO_2 from mineralization plant *j* to cement plant *c*:

$$\begin{aligned} GHG^{avoidedbyCCU}_{c,j} &= GHG^{Cementproduction} \cdot Mass^{UtilizedSiO2}_{c,j} \\ &- \left(GHG^{SolidTransport} \cdot D_{c,j} \cdot Mass^{UtilizedSiO2}_{c,j}\right). \end{aligned} \tag{6}$$

$GHG^{Cementproduction}$ are the GHG emissions caused by production of 1 ton conventional cement. $Mass^{UtilizedSiO2}_{c,j}$ is the amount of SiO_2 that is utilized if we transfer SiO_2 from CO_2 sink *j* to cement plant *c*. This mass is assumed to replace the same mass of conventional cement. $D_{c,j}$ is the distance of the mineralization plant *j* to the utilization site *c*, i.e., cement plant *c*. $GHG^{SolidTransport}$ are the GHG emissions due to transporting 1 ton material for 1 km by truck (see ESI Section S3). The variable $W_{c,j} \in [0,1]$ in the objective function indicates whether and to what extent SiO_2 from the mineralization plant *j* is utilized at the cement plant *c*.

iii) *Storage of excess silicate.* The excess SiO_2 of mineralization plant *j* is transported back to the same mine that supplies the solid feedstock to mineralization plant *j*, to be stored permanently. $D^{ToStorage}_j$ is the distance of the mineralization plant *j* to the location of mine for refilling. The variable $Mass^{ExcessSiO2}_j \in R^+$ indicates the amount of SiO_2 that is produced at mineralization plant *j* but not utilized in a cement plant (see Equation (8)).

iv) *Site construction* . $GHG^{SiteConstruction}$ quantifies the GHG emissions due to the preparation and construction of the site for a new open-pit mine and a new mineralization plant (see ESI Section S3 and Table S5). The binary variable $Z_j \in \{0,1\}$ indicates whether a CO_2 mineralization plant and corresponding mine are constructed at location *j*.

To model the CCUS supply chain, we define three types of constraints *a) Plant size, b) Mass balance, and c) Transport distance.* We select the constraints based on physical or operational limits, such as the maximum extraction capacity of the solid feedstock or the maximum transport distance of bulk materials.

a) *Plant size constraints.* The maximum size of a mineralization plant ($Size^{Max}_j$) is limited to the maximum extraction capacity of the solid feedstock source that supplies the mineralization plant *j* (10 Mt minerals/year for the *base-case scenario,* see Section 2.1).

Our factory construction and mine construction data are based on industrial-scale plants and do not represent small-scale plants. Thus, a mineralization plant should at least mineralize $Size^{Min}_j = 1\ Mt\ CO_2/year$, which is the CO_2 emission of an average cement plant in Europe (European Cement Research Academy, 2017). Noteworthy, the minimum plant size ($Size^{Min}_j$) has only limited effect on the CCUS supply chain (see ESI Section S2).

Hence, if CO_2 mineralization plant *j* is built, the amount of supplied CO_2 to plant *j* has to be larger than $Size^{Min}_j$ and smaller than $Size^{Max}_j$:

$$Size^{Min}_j \cdot Z_j \le \sum_{i\in I}\left(\lceil Y_{i,j}\rceil \cdot F_i\right) \le Size^{Max}_j \cdot Z_j \qquad \forall j \in J. \tag{7}$$

$\lceil Y_{i,j}\rceil$ is zero ($\lceil Y_{i,j}\rceil = 0$) only if $Y_{i,j} = 0$. $\lceil Y_{i,j}\rceil$ is one ($\lceil Y_{i,j}\rceil = 1$) if $Y_{i,j} > 0$.

b) *Mass-balance constraints.*

SiO_2 mass balance. The byproduct SiO_2 cannot be accumulated in a mineralization plant. Thus, excess SiO_2 is the mass of SiO_2 that is produced in CO_2 sink *j* minus the mass of SiO_2 from CO_2 sink *j* that is utilized in cement plants. The excess mass of SiO_2 is backfilled in the solid feedstock mine.

$$\sum_{i,c\in I}\left(Y_{i,j} \cdot Mass^{ProducedSiO2}_{i,j} - W_{c,j} \cdot Mass^{UtilizedSiO2}_{c,j}\right) = Mass^{ExcessSiO2}_j \qquad \forall j \in J \tag{8}$$

$Mass^{ProducedSiO2}_{i,j}$ is the amount of SiO_2 that is produced if CO_2 from CO_2 source *i* is supplied to CO_2 sink *j*.

Furthermore, since a higher substitution rate than 20 wt% could reduce the performance of the cement, the amount of utilized SiO_2 in cement plant *c* must be lower than 20 wt% of the produced cement in cement plant *c*:

$$\sum_{j\in J} W_{c,j} \cdot Mass^{UtilizedSiO2}_{c,j} \le 0.2 \cdot Mass^{Cement}_c \qquad \forall\, i, c \in I \tag{9}$$

$Mass^{Cement}_c$ is the amount of cement produced in cement plant *c* before substitution.

CO_2 mass balance. The CO_2 transferred from CO_2 source *i* must not be higher than the available CO_2 in CO_2 source *i*. Thus, the sum of the transferred CO_2 and the avoided CO_2 emission due to cement substitution must be smaller than the available CO_2:

$$F_i \cdot \sum_{j\in J} Y_{i,j} - GHG^{AvoidedbySub} \cdot \sum_{j\in J}\left(W_{c,j} \cdot Mass^{UtilizedSiO2}_{c,j}\right) \le F_i \qquad \forall\, i, c \in I \tag{10}$$

$GHG^{AvoidedbySub}$ are the avoided GHG emissions due to substituting 1 ton clinker of the cement plant.

c) *Transport distance constraints.* The maximum transport distance is limited for both SiO_2 and CO_2.

To avoid recompression stations, we assume that the longest direct distance for a CO_2 pipeline ($D^{LongestCO2}$) is 325 km in line with literature (d'Amore and Bezzo, 2017; Hasan et al., 2015; Hasan et al., 2014; Metz, 2005; Pehnt and Henkel, 2009):

$$D_{i,j} \cdot \lceil Y_{i,j}\rceil \le D^{LongestCO2} \qquad \forall\, i \in I,\ j \in J \tag{11}$$

Increasing the longest direct distance for a CO_2 pipeline ($D^{LongestCO2}$) could increase the GHG emissions reduction potential of a CCUS supply chain. However, increasing the longest CO_2 pipeline not only increases the network's complexity due to recompression stations but also substantially increases the CO_2 network's size (see ESI Section S2). Therefore, to reduce the network's complexity and design a CO_2 network that is comparable with other studies, we limit the CO_2 pipeline distance to 325 km.

The longest distance for SiO_2 transport ($D^{LongestSiO2}$) is the same as for solid feedstock, 500 km (cf. section 2.1):

$$D_{c,j} \cdot \lceil W_{c,j} \rceil \; \leq \; D^{LongestSiO2} \qquad \forall\, c \in C\,,\, j \in J. \tag{12}$$

$\lceil W_{c,j} \rceil$ is zero ($\lceil W_{c,j} \rceil = 0$) only i $= 0$. $\lceil W_{c,j} \rceil$ is one ($\lceil W_{c,j} \rceil = 1$) if $W_{c,j} > 0$. Increasing the longest distance for SiO_2 transport ($D^{LongestSiO2}$) has a limited effect on GHG emissions reduction potential of a CCUS supply chain (see ESI Section S2).

3.2. Second optimization problem: local pipeline network

After matching the CO_2 sources with the CO_2 sinks (CO_2 mineralization plants) in the sink-source matching optimization, the local pipeline network optimization minimizes the GHG emissions due to building and operating the required CO_2 pipeline network for each CO_2 sink. Increasing the CO_2 pipe diameter decreases both the pressure drop and the weight of pipe per ton of CO_2 transferred; consequently, it decreases the GHG emissions due to building and operating the CO_2 network. Therefore, in the local pipeline network optimization, we merge the CO_2 pipes from multiple CO_2 sources into larger-sized pipes to minimize the GHG emissions of the CO_2 network for each CO_2 sink (Middleton and Bielicki, 2009; Zhou et al., 2014). Our local pipeline network optimization is set up according to the MILP optimization model of Zhou et al. (2014) (see Eq. 13 and Table 2).

From the solution of the sink-source matching optimization, we use three pieces of information a) the selected CO_2 sources (i), b) the selected CO_2 sinks (j), and c) the binary parameter $K_{i,j} \in \{0,1\}$ that defines whether the CO_2 source i supplies CO_2 to the CO_2 sink j. The binary parameter $K_{i,j}$ is derived from the results of variable $Y_{i,j}$ of the sink-source matching optimization ($K_{i,j} = \lceil Y_{i,j} \rceil$). If CO_2 source i supplies CO_2 to more than one CO_2 sink, we virtually divide the CO_2 source i into several CO_2 sources according to the $Y_{i,j}$.

The objective function of the local pipeline network optimization minimizes the GHG emissions due to building and operating the required CO_2 pipeline network.

Objective function:

$$\begin{aligned} \min_{H_{i,l,t},\, Mass^{CO2}_{i,l,t}} \sum_{i\varepsilon I}\sum_{l\varepsilon L}\sum_{t\varepsilon T}\Big(& GHG_t^{CO2Transport} \cdot Mass^{CO2}_{i,l,t} \cdot D_{i,l} \\ & + \left(GHG_t^{Pipe} + GHG^{Trenching}\right) \cdot \; H_{i,l,t} \cdot D_{i,l}\Big), \end{aligned} \tag{13}$$

where i is the CO_2 source selected from the sink-source matching optimization; j is the selected CO_2 sink from the sink-source matching optimization; t is the pipe diameter according to standard ASTM A53/A53M ranging from 50 mm to 600 mm; l is either a CO_2 source or a CO_2 sink ($L = I \cup J$). In the local pipeline network optimization, a CO_2 pipeline can connect CO_2 source i either to another CO_2 source i' or to CO_2 sink j. Thus, l presents all possible destinations from a CO_2 source i.

The objective function of the local pipeline network optimization consists of two parts:

Table 2
List of all variables and parameters of the local pipeline network optimization.

Variables	Parameters
$H_{i,l,t}$, $Mass^{CO2}_{i,l,t}$	$D_{i,l}$, $GHG_t^{CO2Transport}$, $D_{i,l}$, GHG_t^{Pipe}, $GHG^{Trenching}$, $K_{i\ j}$, $Mass_t^{maxCO2}$, $Mass_t^{minCO2}$

i) *GHG emissions due to operating the pipeline.* $GHG_t^{CO2Transport}$ is the GHG emissions caused by transport of 1 ton CO_2 in a pipeline of the diameter t, mainly due to energy demand for overcoming the pressure drop (see ESI Section S3). The variable $Mass^{CO2}_{i,l,t} \in R^+$ is the amount of CO_2 that is transported between CO_2 source i and destinations l via a pipeline of diameter t. $D_{i,l}$ is the distance between CO_2 source i and destinations l.

ii) *GHG emissions due to building and installing the pipe.* GHG_t^{Pipe} quantify the GHG emissions per kilometer, caused by the construction and installation of a CO_2 pipeline with a diameter of t (see ESI Section S3). $GHG^{Trenching}$ is the GHG emissions per kilometer caused by trenching and site preparation for installing a CO_2 pipeline (see ESI Section S3). The binary variable $H_{i,l,t} \in \{0,1\}$ indicates whether there is a connection between CO_2 source i and destinations l with a pipeline diameter t.

To model the local pipeline network, we define four types of constraints *a) matching partners, b) pipeline threshold, c) CO_2 mass balance, and d) integerc.*

a) *Matching partners constraints.* The local pipeline network optimization is not allowed to change the results of the sink-source matching optimization. Therefore, to ensure the same matches between CO_2 source i and CO_2 sink j as the sink-source matching optimization, we define the following constraints using binary parameter $K_{i,j} \in \{0,1\}$. The binary parameter $K_{i,j} \in \{0,1\}$ contains the matched pairs of the sink-source matching optimization ($K_{i,j} = \lceil Y_{i,j} \rceil$), and thus $K_{i,j}$ defines whether the CO_2 source i supplies CO_2 to the CO_2 sink j.

Only if CO_2 source i and CO_2 source i' supply CO_2 to the same CO_2 sink j, the two CO_2 sources can be connected with a pipe pipeline diameter of t:

$$\sum_{t\in\, T} H_{i,i',t} \leq \sum_{j\in\, J}\left(K_{i\ ,j} \cdot K_{\ i',j}\right) \qquad \forall\, i, i' \in I \tag{14}$$

The binary variables $H_{i,l,t} \in \{0,1\}$ indicates whether there is a connection between CO_2 source i and destinations l via pipeline diameter of t.

Only if CO_2 source i supplies CO_2 to CO_2 sink j, the CO_2 source i can be connected to CO_2 sink j with a pipe pipeline diameter of t:

$$\sum_{t\in\, T} H_{i,j,t} \leq K_{\ i\ ,j} \qquad \forall\, i \in I,\ j\ \in J \tag{15}$$

b) *Pipeline threshold constraints.* The model ensures the operation of the CO_2 pipes within the pipeline operating threshold:

$$H_{i\ ,l\ ,t} \cdot Mass_t^{minCO2} \;\leq Mass^{CO2}_{i,l,t} \leq H_{i\ ,l\ ,t} \cdot Mass_t^{maxCO2} \qquad \forall\, i \in I,\ l\ \in L,\ t \in T \tag{16}$$

$Mass_t^{maxCO2}$ and $Mass_t^{minCO2}$ are the maximum and minimum mass flow allowed in a pipeline with a diameter of t, respectively. $Mass_t^{maxCO2}$ and $Mass_t^{minCO2}$ are imposed by maximum and minimum fluid velocity (ASTM A53/A53M, 2012; Wildbolz, 2007). We follow the common assumption that the CO_2 fluid velocity is between 1 and 3 m/s (Wildbolz, 2007).

c) CO_2 mass-balance constraints. CO_2 cannot be stored at a CO_2 source i. Therefore, for each selected CO_2 source i, the sum of all CO_2 masses arriving from another CO_2 source i' ($Mass^{CO2}_{i',i,t}$), leaving to another CO_2 source i'' ($Mass^{CO2}_{i,\, i'',t}$), or to CO_2 sink j ($Mass^{CO2}_{i,j,t}$) via all pipe diameters t plus the captured CO_2 emissions at the CO_2 source i (F_i) should be equal to zero. This constrain is reflected in the mass balance for CO_2:

$$0 = \sum_{t\in T}\left(\sum_{i'\in I}\left(Mass^{CO2}_{i',i,t} - Mass^{CO2}_{i,i'',t}\right) - \sum_{j\in J} Mass^{CO2}_{i,j,t}\right) + F_i \qquad \forall\, i \in I \tag{17}$$

F_i is the amount of captured CO_2 from source *i*.

d) *Integer constraints.* The following constraints (Equations (18)–(20)) ensure that in the network, no round, two-way, or double connection occur:

$$H_{i,i,t} = 0 \qquad \forall\, i \in I,\ t \in T \tag{18}$$

$$H_{i,i',t} + H_{i',i,t} \leq 1 \qquad \forall\, i, i' \in I,\ t \in T \tag{19}$$

$$\sum_{t\in T} H_{i,l,t} \leq 1 \qquad \forall\, i \in I,\ l \in L \tag{20}$$

In our study, we do not consider geographical or political constraints. Rivers, mountains, or national borders, i.e., geographical or political constraints, can substantially change the configuration of CO_2 pipeline network. Yet, the exact configuration of CO_2 pipeline network has a small contribution to the total GHG emissions of a CCUS supply chain (Middleton and Bielicki, 2009). Thus, the effect of exact network configuration on our results is expected to be negligible. This expectation is confirmed by the results shown below where the CO_2 network only contributes 2 % to the total GHG emissions. As alternative CO_2 supply options, without building a CO_2 pipeline network, we analyze direct air capture (DAC) and CO_2 transport by trucks in section 4.

We implement the mathematical optimization problems of Sections 3.1 and 3.2 together with the background data of Section 2 in Python™ (Python Software Foundation, 2019) and solve the resulting mixed-integer linear program (MILP) optimization model using the Gurobi™ Optimizer (Gurobi Optimization, 2020).

4. Results and discussion

In section 4.1, we discuss the results of the base-case scenario and derive the large-scale potential of CCUS by CO_2 mineralization supply chain. Section 4.2 defines five additional scenarios on CO_2 supply, energy supply, and feedstock availability to analyze the supply chain of CCUS by CO_2 mineralization.

4.1. GHG mitigation potential of CCUS by mineralization supply chain

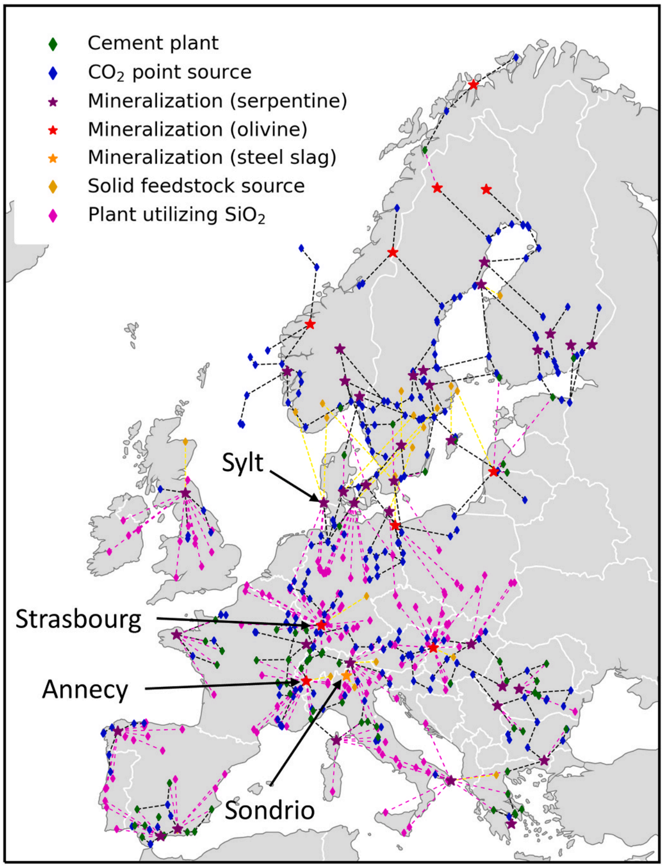

Fig. 5. Climate-optimal supply chain of CO_2 capture, utilization, and storage by mineralization in Europe for the base-case scenario. For co-located mineralization plants and solid feedstock sources, we only illustrate the mineralization plant.

By applying our optimization model, we design the climate-optimal CCUS by mineralization supply chain. The *base-case scenario* estimates the potential of CO_2 mineralization for GHG emissions reduction in Europe. The supply chain captures CO_2 from the industrial sector, uses active and potential locations for natural solid feedstock as well as steel slag (cf. Section 2.1). Furthermore, the supply chain operates using the current national electricity grid mix and obeys the constraints given in section 3.

For the base-case scenario, the supply chain captures 179 Mt CO_2/year and avoids 130 Mt CO_{2e}/year. Thus, the CCUS supply chain for the

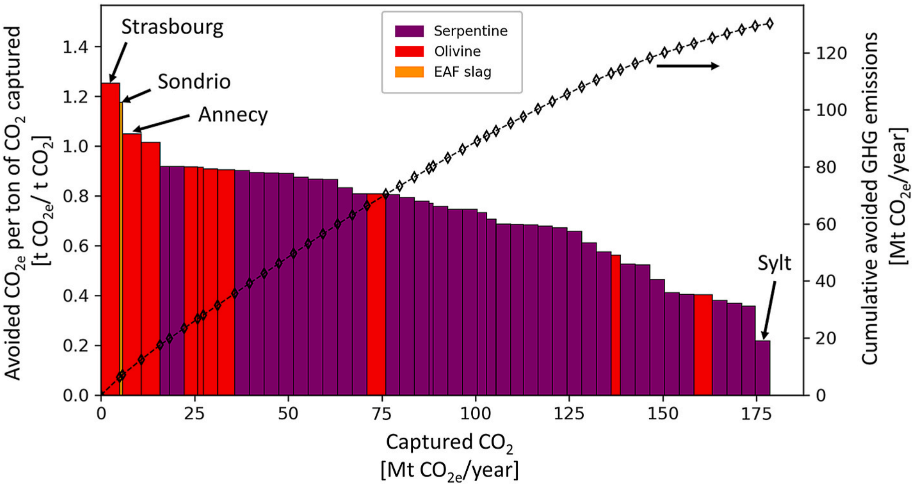

Fig. 4. Climate-merit-order curve for avoided CO_{2e} per ton of CO_2 captured over the captured CO_2 for the base-case scenario. Each bar indicates a mineralization plant. The dashed line shows the cumulative avoided GHG emissions per year over the captured CO_2 per year. Colors indicate the solid feedstock.

base-case scenario could reduce 24 % of the industry sector's GHG emissions in Europe (Fig. 4). Around 20 Mt CO_{2e} avoided/year is due to the utilization of mineralization byproducts (SiO_2) in the cement industry (see Fig. 6 and ESI Section S1). The supply chain for the *base-case scenario* causes indirect emissions of around 69 Mt CO_{2e}/year. Energy demand, solid transport, and CO_2 transportation contribute 72 %, 13 %, and 2 % to the indirect GHG emissions, respectively.

Here, we discuss four outstanding mineralization plants close to "Strasbourg", "Sondrio", "Annecy", and "Sylt".

The avoided CO_{2e} per ton of CO_2 captured ranges from 1.25 ton CO_{2e} avoided/ton CO_2 captured for "Strasbourg" to 0.22 ton CO_{2e} avoided/ton CO_2 captured for "Sylt" (Figs. 4 and 5). This variation is mainly due to a) different national electricity grid mix and b) the portion of SiO_2 utilized in cement production from each mineralization plant. The mineralization plant "Strasbourg" utilizes 99 wt% of the produced $SiO_{2,}$ while the mineralization plant "Sylt" utilizes 21 wt% of its produced $SiO_{2.}$ The avoided CO_{2e} per ton of CO_2 captured plant can even exceed 1 ton CO_{2e} avoided per ton CO_2 captured when a high share of the produced SiO_2 substitutes cement (see Fig. 4 and ESI Section S1, *Pure CCS scenario*).

The mineralization plant sizes vary substantially, ranging from 5 Mt CO_{2e} captured/year for "Annecy" to 0.7 Mt CO_{2e} captured/year for "Sondrio" (Figs. 4 and 5). The mineralization plant size is mainly determined by the extraction capacity of solid feedstock and the availability of close-by CO_2 sources. For instance, the mineralization plant "Annecy", located in France, benefits from a potentially large olivine mine and mineralizes CO_2 from several CO_2 sources in France, Italy, and Switzerland.

CO_2 mineralization plants of the CCUS by mineralization supply chain are not distributed uniformly in Europe. Due to the high availability of CO_2 sources, several large-scale CO_2 mineralization plants are located in the northwest of Germany and in the east of France (Fig. 5).

The potentially available solid feedstocks in Sweden, Finland, and Norway are expected to be sufficient to mineralize the entire CO_2 emissions of these three countries. The excess solid feedstock is transported to supply mineralization plants, mineralizing CO_2 emissions from Germany, Poland, Latvia, Estonia, Denmark, and the Netherlands (Fig. 5).

In summary, large mineralization plants with a high rate of CO_{2e} avoided per CO_2 captured are located, where both CO_2 point sources and solid feedstock are largely available.

4.2. Supply chain of CCUS by mineralization

The CCUS supply chain for the *base-case scenario*, which could avoid 130 Mt CO_{2e}/year, is based on four elements:

a) *169* TWh electricity demand and 88 TWh thermal energy demand,
b) *31,000* km of CO_2 pipeline network, to collect CO_2 emissions from *322* CO_2 sources,
c) *47* large-scale CO_2 mineralization plants, and
d) *47* large-scale mines providing natural solid feedstock.

This section analyzes the importance of the four elements and their effect on both the GHG reduction potential of CCUS by mineralization and the supply chain configuration. For this purpose, we define five alternative scenarios on CO_2 supply, energy supply, and feedstock availability (see Table 3). The supply chain of CCUS by mineralization and the corresponding climate-merit-order curve of all considered scenarios are presented in ESI Section S1.

4.2.1. Energy supply

169 TWh of electricity demand and 88 TWh of natural gas demand for heat correspond to 5.2 % and 2 %, respectively, of the European consumption in 2018 (Agora Energiewende and Sandbag, 2019; Eurostat, 2020a). The energy demand stems mainly from the energy-intensive processes of CO_2 capture and CO_2 mineralization. The energy demands due to CO_2 transport and feedstock mining are smaller. Powerplants with a capacity of 20 GW would be needed to supply the required electricity.

According to the International Energy Agency (IEA), the electricity of Europe will be supplied via 60 % renewable and 40 % non-renewable sources while electricity production increases by 7 % in the year 2040 (IEA, 2018). Thus, the carbon footprint of the European grid mix in 2040 decreases by 70 % from 400 to 114 gr CO_{2e}/kWh. By 2040 the entire thermal heat energy demand could be electrified, as electric heating's carbon footprint will be lower than natural gas combustion. CO_2 capture and mineralization are energy-intensive (Ostovari et al., 2020). Therefore, decreasing the carbon footprint of the energy supply decreases the indirect GHG emissions of the CCUS supply chain and, thus, increases the avoided GHG emissions by 20 % compared to the *base-case scenario* (see *low-emission energy scenario* in ESI section S1, Fig. 6, and Table 4). The required electricity demand of the *low-emission energy scenario* amounts to 7.5 % of the entire electricity production of Europe in 2040 or 12 % of available renewable electricity in Europe by 2040 (IEA, 2018).

The total energy (electricity and natural gas) demand of the CCUS supply chain for the *base-case* scenario corresponds to less than 10 % of the available electricity of Europe. To have a comparable energy demand for all scenarios, we limit the CCUS supply chain's electricity demand of the *carbon-negative scenario* to 10 % of the available electricity in Europe by 2040 (see ESI Section S1 and S6). While the available electricity does not affect the total GHG reduction potential of all other scenarios, the GHG reduction potential of the *carbon-negative scenario* depends strongly on the available electricity.

Our assessment shows that the required energy for the CCUS supply

Table 3
Summary of the six main scenarios. For extraction capacity of active mines, see ESI section S5.

Scenario name	Energy supply	CO_2 sources	CO_2 transport method	Natural solid feedstock locations	Mine extraction capacity [Mt minerals/year]
Base-case	*Current energy mix*	*Industry*	*Pipeline*	*Active & potential*	*10*
Low-emission energy	***Europe 2040***	*Industry*	*Pipeline*	*Active & potential*	*10*
CO_2 road transport	*Current energy mix*	*Industry*	***Truck***	*Active & potential*	*10*
Carbon-negative	***Europe 2040***	***Direct air capture***	-	*Active & potential*	*10*
Current solid feedstock	*Current energy mix*	*Industry*	*Pipeline*	***Only active***	***Depends on mine***
Low-extraction- capacity	*Current energy mix*	*Industry*	*Pipeline*	*Active & potential*	***2.5***

chain could be supplied either by expanding the current energy system or, favorably, by developing renewable energy in the future.

4.2.2. CO_2 supply

The *31,*000 km CO_2 pipelines in Europe correspond to less than 16 % of the 200,000 km high-pressure natural gas pipelines existing in Europe today (Papadakis, 2005). Our results are comparable with the study of d'Amore et al. on a European supply chain for CO_2 capture, transport, and geological storage (d'Amore and Bezzo, 2017). By dividing Europe into 124 cells, ranging from 123 km to 224 km, d'Amore et al. designed an economically optimal supply chain to capture around 845 Mt CO_2/year while moving CO_2 for more than 24,000 km. Our study designs a climate-optimal supply chain and locates all CO_2 sources and sinks with 5 km precision; therefore, the required CO_2 network of our study is larger. Importantly, the required CO_2 network should not be exclusive for CCUS by mineralization but can be shared by other means of carbon capture and storage or utilization.

Still, due to high population density, nature conservation areas, and social acceptance, implementing a CO_2 pipeline network in Europe can be challenging (Wuppertal Institute, 2018). If a CO_2 pipeline network cannot be built, CO_2 can be transported by trucks or even supplied by locally installed direct air capture (DAC).

Transporting the 179 Mt captured CO_2 for the maximum distance of 325 km, increases the total road freight transport of Europe (1,922,933 Mt·km) by less than 3 % (Eurostat, 2020b). However, transporting CO_2 by trucks increases the transport emissions by about 2 Mt CO_{2e}/year (Fig. 6 and Table 4). Thus, the GHG mitigation of the CCUS supply chain slightly decreases to 128 Mt CO_{2e} avoided/year, i.e., 1.5 % reduction compared to the *base-case scenario* (see *CO_2 road transport scenario* ESI Section S1). Yet, the economic and social aspects of CO_2 transport by trucks can be critical for its implementation.

Direct air capture (DAC) plants are another potential technology to supply the required CO_2 without building a CO_2 pipeline network (see *carbon-negative scenario* ESI Section S1 and S6). For the *carbon-negative scenario,* the supply chain uses the electricity grid mix of 2040 and captures exclusively from the atmosphere via DAC. The supply chain could capture 185 Mt CO_2/year and avoid 160 Mt CO_{2e}/year; thereof, around 24 Mt CO_{2e} avoided/year is due to utilization of mineralization byproducts in the cement industry (see Fig. 6). The remaining 136 Mt CO_{2e} per year are carbon negative (Fig. 6). The CO_2 captured via DAC and stored by CO_2 mineralization is removed permanently from the atmosphere and is carbon negative.

In summary, the required CO_2 can be supplied by three options a) a new infrastructure for CO_2 pipeline network that can be shared with other CCU/CCS approaches, b) an already available infrastructure for truck road freight transportation, or c) direct air capture technology that can provide negative emissions in the future.

4.2.3. Large-scale mineralization plant

Although there have been several developments to scale up CO_2 mineralization, the technology is still at the pilot plant scale (Veetil and Hitch, 2020). Our work is, therefore, a "tomorrow's technology today" study. We assume that the laboratory scale performance of CO_2 mineralization represents the future industrial-scale plant (Tanzer et al., 2020). Nonetheless, large-scale mineralization plants are a critical element for the supply chain of CCUS by mineralization. In section 5, we discuss several approaches to accelerate the development of mineralization technology.

4.2.4. Large-scale mineral deposits

The *base-case scenario* employs 47 large-scale natural mineral mines. Currently, only 5 locations are active. To estimate the GHG emissions reduction potential of the currently active solid feedstock locations, we define the *current solid feedstock scenario* that uses the five currently active natural mineral mines at the current extraction rates *(Kremer et al., 2019)* and all available EAF steel slag. Here, we assume that the entire market for natural mineral mines could be used for CO_2 mineralization. The supply chain for the *current solid feedstock scenario* could avoid 4.8 Mt CO_{2e}/year, i.e., only 3.6 % of the *base-case scenario*'s potential (see Fig. 6 and ESI Section S2). Thus, new mines are needed to exploit the large potential.

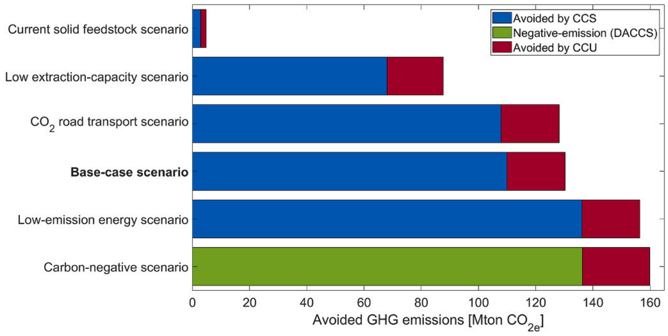

Fig. 6. Avoided greenhouse gas (GHG) emission of CCUS by mineralization supply chain for the six main scenarios (cf. Table 3). CCS is carbon capture and storage. DACCS is direct air capture with carbon storage. CCU is carbon capture and utilization.

To investigate the effect of solid feedstock extraction capacity, we define the *low extraction-capacity scenario. The low extraction-capacity scenario* allows to use all potential locations for solid feedstock but only at *25 % of assumed extraction capacity* (i.e., 2.5 Mt minerals/year) for natural minerals. The supply chain for the *low extraction-capacity scenario* captures 96 Mt CO_2/year and avoids 88 Mt CO_{2e}/year, i.e., 67 % of the *base-case scenario's* potential (see Fig. 6, Table 4, and ESI Section S2).

The results of the *current solid feedstock scenario and the low extraction-capacity scenario* show that both the availability and the extraction capacity of the natural mineral mines are essential to reach the GHG mitigation of the *base-case scenario* (130 Mt CO_{2e}/year). Hence, an investigation is crucial to determine the availability of the potential natural mineral mines and to scale up the extraction capacity.

Fig. 6 and Table 4 illustrate the avoided greenhouse gas (GHG) emissions of CCUS by mineralization supply chain for the six main scenarios mentioned in Table 3. The selection of a scenario depends substantially on uncertain parameters imposed externally, such as the availability of low-emission electricity or the extraction capacity of solid feedstock, etc. The carbon-negative scenario has the largest GHG emission reduction potential (160 Mt CO_{2e}/year). A detailed illustration of results for all scenarios is presented in ESI Section S1.

4.3. Non-climate environmental impacts

Our study mainly focuses on the climate change impact of a CCUS by CO_2 mineralization supply chain. However, it is essential to assess other environmental impact categories to avoid problem shifting to other impact categories (Miller and Moore, 2020). For this purpose, we use the *ReCiPe 2016* life cycle impact method (Huijbregts et al., 2017). We illustrate change in the environmental impacts of CCUS by mineralization supply chain for the base-case scenario and the base-case scenario using wind energy in Fig. 7.

The CCUS by CO_2 mineralization supply chain of the *base-case scenario* increases 12 out of 19 environmental impacts except for climate change. The increase is mainly due to increased energy demand (Miller and Moore, 2020) and increased resource consumption (Baumgärtner et al., 2021).

The results of the base-case scenario show that implementing CCUS by mineralization supply chain in Europe could decrease the GHG emission of the industry sector in Europe by 24 %, i.e., 130 Mt CO_{2e}/year. The 130 Mt CO_{2e}/year corresponds to about 0.2 % of the climate change impact of the entire world, including all continents and all

Table 4
Summary of the results of the six main scenarios. A detailed illustration of results for all scenarios is presented in ESI Section S1.

Scenario name	*Avoided GHG emission [Mt CO_{2e}/year]*	Electricity demand [TWh]	*Thermal energy demand [TWh]*	CO_2 pipeline [km]	Nr. of natural mineral mines
Base-case	*130*	*169*	*88*	*~31,000*	*47*
Low-emission energy	*156*	*261*	*0*[a]	*~31,000*	*49*
CO_2 road transport	*128*	*171*	*88*	*0*	*49*
Carbon-negative	*160*	*350*	*0*[a]	*0*	*46*
Current solid feedstock	*4.8*	*4*	*88*	*~1300*	*2*
Low-extraction- capacity	*88*	*110*	*17*	*~36,000*	*93*

[a] The entire thermal heat demand is supplied by electric heating.

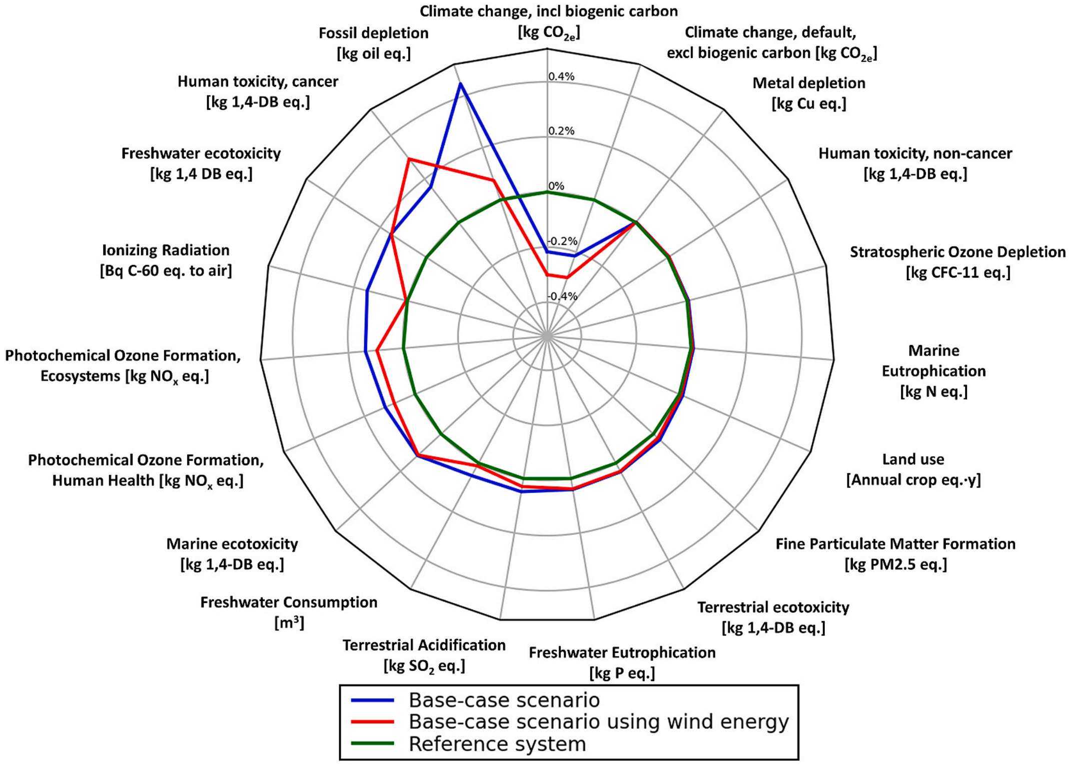

Fig. 7. Change in environmental impacts of CCUS by mineralization supply chain for the base-case scenario and the base-case scenario using wind energy. The reference system is the environmental impact of the world.

sectors. Estimating the global GHG reduction potential of CCUS by mineralization requires analyzing the implementation of CO_2 mineralization supply chain in all continents.

We can use this 0.2 % decrease in global climate change impact to assess the trade-off with other environmental impacts. While CCUS by mineralization reduces GHG emissions, its energy demand increases the fossil-fuel-related environmental impacts, such as fossil depletion and ionizing radiation impacts, could increase by about 0.4 % and 0.18 %, respectively. Using wind energy to operate the CCUS supply chain could limit or even remove the increase in fossil-fuel-related environmental impacts (Fig. 7). The results indicate the co-benefit of decarbonizing the electricity supply to reduce the environmental impacts of CCUS by mineralization. To decrease the resource-consumption-related environmental impacts, CO_2 capture and mineralization technologies should be further improved.

The high impact for "human toxicity, cancer" stems from a generic dataset for factory construction of CO_2 mineralization where the required copper production leads to high impacts. The qualitative and quantitative impacts of copper production for factory construction need to be carefully quantified for an actual implementation (see ESI Section S3).

Our model designs the CCUS supply chain by maximizing GHG emissions mitigation and neglects other environmental trade-offs. For designing a simultaneously optimized CCUS supply chain, a multi-objective optimization model is required. This could be the subject of future work.

5. Conclusions

In our study, by applying an optimization model, we present a climate-optimal supply chain for CO_2 capture, utilization, and storage by mineralization in Europe. We quantify the potential of CO_2 mineralization for GHG emissions reduction and analyze the required supply chain to achieve the GHG emissions reduction.

For the *base-case scenario*, the supply chain of CO_2 mineralization can avoid 130 Mt CO_{2e}/year in Europe, i.e., a 24 % reduction of the industry sector's GHG emissions. Furthermore, by combining direct air capture (DAC) and low-emission energy supply, the CCUS supply chain can provide negative emissions at a rate of 136 Mt CO_{2e}/year. Thus, a CO_2 mineralization supply chain could reduce GHG emissions from the current industry sector and act as a carbon-negative technology in the future.

The required CO_2 and energy for the CCUS supply chain can be supplied, either by expanding the existing infrastructure, i.e., road freight transportation and current energy mix, or by building new infrastructure in the future, i.e., CO_2 pipeline network, DAC, and renewable electricity system. One promising transition path is to start small and flexible, i.e., using the existing energy system to capture CO_2 from the industrial point sources, and transport the captured CO_2 by the currently available truck road transportation infrastructure. The supply chain for CCUS by mineralization could, thus, be gradually developed and fully implemented in the future to provide negative emissions on a large scale via direct air capture.

Still, to achieve the CCUS supply chain's high potential for GHG emissions reduction, two critical elements are required a) large-scale CO_2 mineralization plants and b) large-scale mineral deposits.

The first critical element is the CO_2 mineralization technology that is still at the pilot scale. To further develop CO_2 mineralization technology toward commercialization, a sound economic business case is required. Value could be created by increasing the revenue of CO_2 mineralization, e.g., utilizing a large portion of mineralization byproducts in the cement market. To maximize the revenue from byproducts sales, the locations close to both cement plants and currently active solid feedstock mines are favorable, e.g., Italy, Spain, and Greece. Another source of revenue could be utilizing the main product of mineralization (carbonates) in industry and substitute conventional products. Substituting conventional products with carbonates increases both the economic and the environmental potential. Furthermore, governmental regulations, such as financial aids from the European innovation fund or incentivizing emissions reduction in the European emissions trading system (EU ETS), could foster the economic business case of mineralization. Understanding the economics of CCUS by mineralization requires designing an economically optimal supply chain. For this purpose, the objective function of the optimization problem should be the total cost of the supply chain. Our study illustrates that a large-scale CCUS by mineralization could reduce GHG emissions, yet, the economic aspects of the supply chain should be the subject of future research.

The second critical element is the required large-scale mineral deposits. The current available solid feedstock could already mitigate 4.8 Mt CO_{2e}/year, but this potential corresponds to only 3.6 % of the *base-case scenario*'s potential. The extraction capacity of the currently active mines could be increased to cover the demand of the new CO_2 mineralization plants. However, both extraction capacity and new locations of solid feedstock are shown to be necessary for large-scale CCUS by mineralization supply chain. Therefore, opening new mines at promising locations for natural solid feedstock should be evaluated. The currently known promising locations are close to several cement plants or other industrial CO_2 point sources, e.g., in the northwest of Germany or in the east of France. Besides technical developments, local governments could foster the commissioning of new mines by accelerating the permission process. Yet, commissioning of new mines should include a critical review of possible direct and indirect environmental impacts, considering indirect land-use change, biodiversity, etc.; thus, avoid shifting the problem from climate change to other environmental impacts.

Open-pit mining has been criticized by society and is highly debated. Hence, the social acceptance of mining for GHG emissions reduction should be evaluated as early as possible (Strunge et al., 2022). An alternative to mining for supplying the required natural solid feedstock is utilizing alternative solid feedstock, such as industrial byproducts or demolished concrete (Meng et al., 2021; Tiefenthaler et al., 2021). The compatibility and availability of the alternative solid feedstock for CO_2 mineralization should be analyzed.

Implementing CCUS by mineralization on a large scale leads to environmental trade-offs that could be limited by decarbonizing the energy supply. However, the effect of energy supply on CO_2 mineralization is much smaller than for other CCU technologies producing chemicals or fuels due to their higher energy demand (Artz et al., 2018). Furthermore, the products of most CCU technologies store CO_2 only temporarily (Müller et al., 2020; von der Assen et al., 2013). Thus, CO_2 mineralization seems particularly promising to reduce GHG emissions.

Similar to CO_2 mineralization, CO_2 capture and geological storage can permanently store CO_2 even with lower energy demand. Yet, CO_2 mineralization could offset its higher energy demand by utilizing its products. Infrastructure for CO_2 mineralization and geological storage could be jointly developed, leading to synergistic cost reductions. Such options could be explored in multi-objective optimization of the mineralization process and the environmental impacts (Fazlinezhad et al., 2022; Hazrati-Kalbibaki et al., 2020; Zhang et al., 2020). Such a multi-objective model could consider several CCUS technologies and CO_2 mineralization to deepen our understanding of CO_2 mineralization and other CCUS technologies on a large scale.

Our study shows that the CCUS by mineralization supply chain could reduce the GHG emissions of industry in Europe by up to 160 Mt CO_{2e} avoided/year. However, the first steps to unlock the high potential of CO_2 mineralization in Europe are scaling up the CO_2 mineralization technology to the industrial level and exploiting large-scale solid feedstocks such as natural mineral deposits or industrial byproducts.

CRediT authorship contribution statement

Hesam Ostovari: Conceptualization, Methodology, Validation, Formal analysis, Investigation, Data curation, Writing – original draft, Writing – review & editing, Visualization. **Leonard Müller:** Methodology, Writing – review & editing. **Fabian Mayer:** Methodology, Writing – review & editing. **André Bardow:** Conceptualization, Funding acquisition, Methodology, Writing – review & editing, Supervision.

Declaration of competing interest

The authors declare that they have no known competing financial interests or personal relationships that could have appeared to influence the work reported in this paper.

Acknowledgment

This work has been carried out within the project "CO2MIN" (033RC014). The project is funded by the German Federal Ministry of Education and Research (BMBF). For the continuous support and cooperation, we would like to thank Luis Kuhrmann, Dario Kremer, Hannah Minten, and our project partners from RWTH Aachen, IASS Potsdam, and HeidelbergCement AG.

Appendix A. Electronic Supporting Information

Electronic Supporting Information to this article can be found online at https://doi.org/10.1016/j.jclepro.2022.131750.

References

Agora Energiewende, Sandbag, 2019. The European Power Sector in 2018. Up-To-Date Analysis on the Electricity Transition.

AlArab, A., Hamad, B., Chehab, G., Assaad, J.J., 2020. Use of ceramic-waste powder as value-added pozzolanic material with improved thermal properties. J. Mater. Civ. Eng. 32, 4020243 https://doi.org/10.1061/(ASCE)MT.1943-5533.0003326.

Artz, J., Müller, T.E., Thenert, K., Kleinekorte, J., Meys, R., Sternberg, A., Bardow, A., Leitner, W., 2018. Sustainable conversion of carbon dioxide: an integrated review of catalysis and life cycle assessment. Chem. Rev. 118, 434–504. https://doi.org/10.1021/acs.chemrev.7b00435.

ASTM A53/A53M, 2012. Standard Specification for Pipe, Steel, Black and Hot-Dipped, Zinc-Coated, Welded and Seamless (A53/A53M).

Baumgärtner, N., Deutz, S., Reinert, C., Nolzen, N., Kuepper, L.E., Hennen, M., Hollermann, D.E., Bardow, A., 2021. Life-cycle assessment of sector-coupled national energy systems: environmental impacts of electricity, heat, and transportation in Germany till 2050. Front. Energy Res. 9, 621502 https://doi.org/10.3389/fenrg.2021.621502.

Benhelal, E., Rashid, M.I., Holt, C., Rayson, M.S., Brent, G., Hook, J.M., Stockenhuber, M., Kennedy, E.M., 2018. The utilisation of feed and byproducts of mineral carbonation processes as pozzolanic cement replacements. J. Clean. Prod. 186, 499–513. https://doi.org/10.1016/j.jclepro.2018.03.076.

Benhelal, E., Oliver, T.K., Farhang, F., Hook, J.M., Rayson, M.S., Brent, G.F., Stockenhuber, M., Kennedy, E.M., 2020. Structure of silica polymers and reaction mechanism for formation of silica-rich precipitated phases in direct aqueous carbon mineralization. Ind. Eng. Chem. Res. 59, 6828–6839. https://doi.org/10.1021/acs.iecr.9b04379.

Bide, T.P., Styles, M.T., Naden, J., 2014. An assessment of global resources of rocks as suitable raw materials for carbon capture and storage by mineralisation. B. Appl. Earth Sci. 123, 179–195. https://doi.org/10.1179/1743275814Y.0000000057.

Bodénan, F., Bourgeois, F., Petiot, C., Augé, T., Bonfils, B., Julcour-Lebigue, C., Guyot, F., Boukary, A., Tremosa, J., Lassin, A., Gaucher, E.C., Chiquet, P., 2014. Ex situ mineral carbonation for CO2 mitigation: evaluation of mining waste resources, aqueous carbonation processability and life cycle assessment (Carmex project). Miner. Eng. 59, 52–63. https://doi.org/10.1016/j.mineng.2014.01.011.

Bremen, A.M., Ploch, T., Mhamdi, A., Mitsos, A., 2021. A mechanistic model of direct forsterite carbonation. Chem. Eng. J. 404, 126480 https://doi.org/10.1016/j.cej.2020.126480.

Bui, M., Adjiman, C.S., Bardow, A., Anthony, E.J., Boston, A., Brown, S., Fennell, P.S., Fuss, S., Galindo, A., Hackett, L.A., Hallett, J.P., Herzog, H.J., Jackson, G., Kemper, J., Krevor, S., Maitland, G.C., Matuszewski, M., Metcalfe, I.S., Petit, C., Puxty, G., Reimer, J., Reiner, D.M., Rubin, E.S., Scott, S.A., Shah, N., Smit, B., Trusler, J.P.M., Webley, P., Wilcox, J., Mac Dowell, N., 2018. Carbon capture and storage (CCS): the way forward. Energy Environ. Sci. 11, 1062–1176. https://doi.org/10.1039/C7EE02342A.

Chen, Z.-Y., O'Connor, W.K., Gerdemann, S.J., 2006. Chemistry of aqueous mineral carbonation for carbon sequestration and explanation of experimental results. Environ. Prog. 25, 161–166. https://doi.org/10.1002/ep.10127.

Chiang, P.C., Pan, Y.S., 2017. Carbon Dioxide Mineralization and Utilizilation. Springer.

d'Amore, F., Bezzo, F., 2020. Optimizing the design of supply chains for carbon capture, utilization, and sequestration in Europe: a preliminary assessment. Front. Energy Res. 8, 190. https://doi.org/10.3389/fenrg.2020.00190.

Davis, S.J., Lewis, N.S., Shaner, M., Aggarwal, S., Arent, D., Azevedo, I.L., Benson, S.M., Bradley, T., Brouwer, J., Chiang, Y.-M., Clack, C.T.M., Cohen, A., Doig, S., Edmonds, J., Fennell, P., Field, C.B., Hannegan, B., Hodge, B.-M., Hoffert, M.I., Ingersoll, E., Jaramillo, P., Lackner, K.S., Mach, K.J., Mastrandrea, M., Ogden, J., Peterson, P.F., Sanchez, D.L., Sperling, D., Stagner, J., Trancik, J.E., Yang, C.-J., Caldeira, K., 2018. Net-zero emissions energy systems. Science 360. https://doi.org/10.1126/science.aas9793.

Deutsches Institut für Normung e. V. Cement - Part 1: Composition, specifications and conformity criteria for common cements; German version (accessed 2011).

Deutz, S., Bardow, A., 2021. Life-cycle assessment of an industrial direct air capture process based on temperature-vacuum swing adsorption. Nat. Energy. https://doi.org/10.1038/s41560-020-00771-9.

d'Amore, F., Bezzo, F., 2017. Economic optimisation of European supply chains for CO 2 capture, transport and sequestration. Int. J. Greenh. Gas Control 65, 99–116. https://doi.org/10.1016/j.ijggc.2017.08.015.

d'Amore, F., Sunny, N., Iruretagoyena, D., Bezzo, F., Shah, N., 2019. Optimising European supply chains for carbon capture, transport and sequestration, including uncertainty on geological storage availability. In: Kiss, A.A. (Ed.), 29th European Symposium on Computer Aided Process Engineering, vol. 46. Elsevier, Amsterdam, pp. 199–204.

d'Amore, F., Romano, M.C., Bezzo, F., 2021. Carbon capture and storage from energy and industrial emission sources: a Europe-wide supply chain optimisation. J. Clean. Prod. 290, 125202 https://doi.org/10.1016/j.jclepro.2020.125202.

Elahi, N., Shah, N., Korre, A., Durucan, S., 2014. Multi-period least cost optimisation model of an integrated carbon dioxide capture transportation and storage infryastructure in the UK. Energy Proc. 63, 2655–2662. https://doi.org/10.1016/j.egypro.2014.11.288.

EUROFER database. European Steel Map. www.eurofer.org.

European Cement Research Academy, 2017. Development of State of the Art Techniques in Cement Manufacturing: Trying to Look Ahead. European Cement Research Academy, Duesseldorf, Geneva. https://ecra-online.org/press-releases/.

EUROPEAN COMMISSION, 2018. Competitiveness of the European Cement and Lime Sectors: Final Report: Directorate General for Internal Market, Industry, Entrepreneurship and SMEs; ECORYS; WIFO. National Institute of Economic and Social Research. Publications Office.

European Environment Agency, 2019. The European Pollutant Release and Transfer Register (E-PRTR). Version 17 (2019 data).

Eurostat, 2020a. Natural Gas Supply Statistics. https://ec.europa.eu/eurostat/statistics-explained/index.php/Natural_gas_supply_statistics. (Accessed 15 June 2020).

Eurostat, 2020b. Summary of Annual Road Freight Transport by Type of Operation and Type of Transport. https://ec.europa.eu/eurostat/databrowser/view/road_go_ta_tott/default/table. (Accessed 24 November 2020).

Fazlinezhad, A., Fattahi, M., Tavakoli-Chaleshtori, R., Rezaveisi, H., 2022. Sensitivity analysis and multi-objective optimization of oxidative dehydrogenation of propane in a fixed-bed reactor over vanadium/graphene for propylene production. Chem. Eng. Technol. 45, 309–318. https://doi.org/10.1002/ceat.202100399.

GaBi 9.2. Software-System and Database for Life Cycle Engineering. thinkstep AG, Leinfelden-Echterdingen, Germany.

Gabrielli, P., Charbonnier, F., Guidolin, A., Mazzotti, M., 2020. Enabling low-carbon hydrogen supply chains through use of biomass and carbon capture and storage: a Swiss case study. Appl. Energy 275, 115245. https://doi.org/10.1016/j.apenergy.2020.115245.

Garrett, T.D., Cardenas, H.E., Lynam, J.G., 2020. Sugarcane bagasse and rice husk ash pozzolans: cement strength and corrosion effects when using saltwater. Curr. Res. Green Sustain. Chem. 1–2, 7–13. https://doi.org/10.1016/j.crgsc.2020.04.003.

Gerdemann, S.J., O'Connor, W.K., Dahlin, D.C., Penner, L.R., Rush, H., 2007. Ex situ aqueous mineral carbonation. Environ. Sci. Technol. 41, 2587–2593. https://doi.org/10.1021/es0619253.

Giannoulakis, S., Kathrin, V., Christian, B., 2014. Life cycle and cost assessment of mineral carbonation for carbon capture and storage in European power generation. Int. J. Greenh. Gas Control 21, 140–157. https://doi.org/10.1016/j.ijggc.2013.12.002.

Gurobi Optimization, 2020. Gurobi Optimizer.

Habert, G., Miller, S.A., John, V.M., Provis, J.L., Favier, A., Horvath, A., Scrivener, K.L., 2020. Environmental impacts and decarbonization strategies in the cement and concrete industries. Nat. Rev. Earth Environ. 1, 1–15. https://doi.org/10.1038/s43017-020-0093-3.

Handbook, I.L.C.D., 2010. International Reference Life Cycle Data System (ILCD) Handbook - General Guide for Life Cycle Assessment. European Commission - Joint Research Centre - Institute for Environment and Sustainability.

Hangx, S.J., Spiers, C.J., 2009. Coastal spreading of olivine to control atmospheric CO2 concentrations: a critical analysis of viability. Int. J. Greenh. Gas Control 3, 757–767. https://doi.org/10.1016/j.ijggc.2009.07.001.

Hasan, M.M.F., Boukouvala, F., First, E.L., Floudas, C.A., 2014. Nationwide, regional, and statewide CO 2 capture, utilization, and sequestration supply chain network optimization. Ind. Eng. Chem. Res. 53, 7489–7506. https://doi.org/10.1021/ie402931c.

Hasan, M.M.F., First, E.L., Boukouvala, F., Floudas, C.A., 2015. A multi-scale framework for CO2 capture, utilization, and sequestration: CCUS and CCU. Comput. Chem. Eng. 81, 2–21. https://doi.org/10.1016/j.compchemeng.2015.04.034.

Seyed Mohsen Hosseini-Ardali, Hazrati-Kalbibaki, Majid, Fattahi, Moslem, Lezsovits, Ferenc, 2020. Multi-objective optimization of post combustion CO2 capture using methyldiethanolamine (MDEA) and piperazine (PZ) bi-solvent. Energy 211, 119035. https://doi.org/10.1016/j.energy.2020.119035.

Hovorka, S., Kelemen, P., 2021. In: Wilcox, J., Kolosz, B. (Eds.), The Building Blocks of CDR Systems: Geological Sequestration, CDR Primer. J Freeman.

Hudson Institute of Mineralogy dba. https://www.mindat.org/.

Huijbregts, M.A.J., Steinmann, Z.J.N., Elshout, P.M.F., Stam, G., Verones, F., Vieira, M., Zijp, M., Hollander, A., van Zelm, R., 2017. ReCiPe2016: a harmonised life cycle impact assessment method at midpoint and endpoint level. Int. J. Life Cycle Assess. 22, 138–147. https://doi.org/10.1007/s11367-016-1246-y.

Huijgen, W.J.J., Ruijg, G.J., Comans, R.N.J., Witkamp, G.-J., 2006. Energy consumption and net CO2 sequestration of aqueous mineral carbonation. Ind. Eng. Chem. Res. 45, 9184–9194. https://doi.org/10.1021/ie060636k.

Hustrulid, W., Kuchta, M., 2006. Open Pit Mine Planning and Design, second ed. Taylor and Francis, London, p. 735.

IEA, 2018. World Energy Outlook. OECD/IEA, [Place of publication not identified], p. 643.

IEA, 2019. Transforming Industry through CCUS. IEA, Paris. www.iea.org/publications/reports/TransformingIndustrythroughCCUS/.

Ince, C., Hamza, A., Derogar, S., Ball, R.J., 2020. Utilisation of waste marble dust for improved durability and cost efficiency of pozzolanic concrete. J. Clean. Prod. 270, 122213 https://doi.org/10.1016/j.jclepro.2020.122213.

IPCC, 2018. Global warming of 1.5°C. An IPCC Special Report on the impacts of global warming of 1.5°C above pre-industrial levels and related global greenhouse gas emission pathways. In: The Context of Strengthening the Global Response to the Threat of Climate Change, Sustainable Development, and Efforts to Eradicate Poverty.

ISO 14040, 2021. Environmental Management - Life Cycle Assessment - Principles and Framework.

ISO 14044, 2021. Environmental Management — Life Cycle Assessment — Requirements and Guidelines.

ISO 14067, 2018. Greenhouse Gases - Carbon Footprint of Products - Requirements and Guidelines for Quantification.

ISO/TR 14049, 2012. Environmental Management — Life Cycle Assessment — Illustrative Examples on How to Apply ISO 14044 to Goal and Scope Definition and Inventory Analysis.

Julcour, C., Bourgeois, F., Bonfils, B., Benhamed, I., Guyot, F., Bodénan, F., Petiot, C., Gaucher, É.C., 2015. Development of an attrition-leaching hybrid process for direct aqueous mineral carbonation. Chem. Eng. J. 262, 716–726. https://doi.org/10.1016/j.cej.2014.10.031.

Kalyanarengan Ravi, N., van Sint Annaland, M., Fransoo, J.C., Grievink, J., Zondervan, E., 2017. Development and implementation of supply chain optimization framework for CO 2 capture and storage in The Netherlands. Comput. Chem. Eng. 102, 40–51. https://doi.org/10.1016/j.compchemeng.2016.08.011.

Kirchofer, A., Becker, A., Brandt, A., Wilcox, J., 2013. CO2 mitigation potential of mineral carbonation with industrial alkalinity sources in the United States. Environ. Sci. Technol. 47, 7548–7554. https://doi.org/10.1021/es4003982.

Kremer, D., Wotruba, H., 2020. Separation of products from mineral sequestration of CO2 with primary and secondary raw materials. Minerals 10, 1098. https://doi.org/10.3390/min10121098.

Kremer, D., Etzold, S., Boldt, J., Blaum, P., Hahn, K.M., Wotruba, H., Telle, R., 2019. Geological mapping and characterization of possible primary input materials for the mineral sequestration of carbon dioxide in Europe. Minerals 9, 485. https://doi.org/10.3390/min9080485.

Lackner, K.S., 2003. Climate change. A guide to CO2 sequestration. Science (New York, N.Y.) 300, 1677–1678. https://doi.org/10.1126/science.1079033.

Lackner, K.S., Wendt, C.H., Butt, D.P., Joyce, E.L., Sharp, D.H., 1995. Carbon dioxide disposal in carbonate minerals. Energy 20, 1153–1170. https://doi.org/10.1016/0360-5442(95)00071-N.

Leonzio, G., Foscolo, P.U., Zondervan, E., 2020. Optimization of CCUS supply chains for some European countries under the uncertainty. Processes 8. https://doi.org/10.3390/pr8080960.

Mattauch, L., Creutzig, F., Edenhofer, O., 2015. Avoiding carbon lock-in: policy options for advancing structural change. Econ. Modell. 50, 49–63. https://doi.org/10.1016/j.econmod.2015.06.002.

Meng, J., Liao, W., Zhang, G., 2021. Emerging CO2-mineralization technologies for Co-utilization of industrial solid waste and carbon resources in China. Minerals 11. https://doi.org/10.3390/min11030274.

Metz, B., 2005. IPCC Special Report on Carbon Dioxide Capture and Storage. Cambridge University Press for the Intergovernmental Panel on Climate Change, Cambridge.

Middleton, R.S., Bielicki, J.M., 2009. A scalable infrastructure model for carbon capture and storage: SimCCS. Energy Pol. 37, 1052–1060. https://doi.org/10.1016/j.enpol.2008.09.049.

Middleton, R.S., Yaw, S.P., Hoover, B.A., Ellett, K.M., 2020. SimCCS: an open-source tool for optimizing CO2 capture, transport, and storage infrastructure. Environ. Model. Software 124, 104560. https://doi.org/10.1016/j.envsoft.2019.104560.

Miller, S.A., Moore, F.C., 2020. Climate and health damages from global concrete production. Nat. Clim. Change. https://doi.org/10.1038/s41558-020-0733-0.

Minerals4EU database. Minerals Intelligence Network for Europe. http://minerals4eu.brgm-rec.fr/.

Morbee, J., Serpa, J., Tzimas, E., 2012. Optimised deployment of a European CO2 transport network. Int. J. Greenh. Gas Control 7, 48–61. https://doi.org/10.1016/j.ijggc.2011.11.011.

Müller, L.J., Kätelhön, A., Bachmann, M., Zimmermann, A., Sternberg, A., Bardow, A., 2020. A guideline for life cycle assessment of carbon capture and utilization. Front. Energy Res. 8, 15. https://doi.org/10.3389/fenrg.2020.00015.

New Boliden. The World's Most Efficient Open-Pit Copper Mine. https://www.boliden.com/operations/mines/boliden-aitik.

Ostovari, H., Sternberg, A., Bardow, A., 2020. Rock 'n' use of CO 2 : carbon footprint of carbon capture and utilization by mineralization. Sustain. Energy Fuels. https://doi.org/10.1039/D0SE00190B.

Ostovari, H., Müller, L., Skocek, J., Bardow, A., 2021. From Unavoidable CO2 Source to CO2 Sink? A Cement Industry Based on CO2 Mineralization. Environmental Science & Technology. https://doi.org/10.1021/acs.est.0c07599.

Pan, S.-Y., Ana Maria, L.L., Pen-Chi, C., 2016. Engineering, environmental and economic performance evaluation of high-gravity carbonation process for carbon capture and utilization. Appl. Energy 170, 269–277. https://doi.org/10.1016/j.apenergy.2016.02.103.

Pan, S.-Y., Chen, Y.-H., Fan, L.-S., Kim, H., Gao, X., Ling, T.-C., Chiang, P.-C., Pei, S.-L., Gu, G., 2020. CO2 mineralization and utilization by alkaline solid wastes for potential carbon reduction. Nat. Sustain. 3, 399–405. https://doi.org/10.1038/s41893-020-0486-9.

Papadakis, G.A., 2005. Overview of pipelines in Europe –advantages and disadvantages. N/ECE Workshop on the Prevention of Water Pollution due to Pipe UN/ECE Workshop on the Prevention of Water Pollution due to Pipeline Accidents. https://www.unece.org/fileadmin/DAM/env/teia/water/pipeline/end_ve_papadakis.pdf.

Pedro, J., Araújo, A.A., Moita, P., Beltrame, M., Lopes, L., Chambel, A., Berrezueta, E., Carneiro, J., 2020. Mineral carbonation of CO2 in mafic plutonic rocks, I—screening criteria and application to a case study in southwest Portugal. Appl. Sci. 10, 4879. https://doi.org/10.3390/app10144879.

Pehnt, M., Henkel, J., 2009. Life cycle assessment of carbon dioxide capture and storage from lignite power plants. Int. J. Greenh. Gas Control 3, 49–66. https://doi.org/10.1016/j.ijggc.2008.07.001.

Picot, J.C., Cassard, D., Maldan, F., Greffié, C., Bodénan, F., 2011. Worldwide potential for ex-situ mineral carbonation. Energy Proc. 4, 2971–2977. https://doi.org/10.1016/j.egypro.2011.02.206.

Power, I.M., Wilson, S.A., Dipple, G.M., 2013. Serpentinite carbonation for CO2 sequestration. Elements 9, 115–121. https://doi.org/10.2113/gselements.9.2.115.

ProMine database. http://promine.gtk.fi/.

Python Software Foundation, 2019. Python: A Dynamic, Open Source Programming Language.

Renforth, P., 2019. The negative emission potential of alkaline materials. Nat. Commun. 10, 1401. https://doi.org/10.1038/s41467-019-09475-5.

Romanov, V., Soong, Y., Carney, C., Rush, G.E., Nielsen, B., O'Connor, W., 2015. Mineralization of carbon dioxide: a literature review. ChemBioEng Rev. 2, 231–256. https://doi.org/10.1002/cben.201500002.

Sanna, A., Matthew, R.H., Mercedes, M.-V., 2012. Post-processing pathways in carbon capture and storage by mineral carbonation (CCSM) towards the introduction of carbon neutral materials. Energy Environ. Sci.

Sanna, A., Uibu, M., Caramanna, G., Kuusik, R., Maroto-Valer, M.M., 2014. A review of mineral carbonation technologies to sequester CO2. Chem. Soc. Rev. 43, 8049–8080. https://doi.org/10.1039/C4CS00035H.

Seto, K.C., Davis, S.J., Mitchell, R.B., Stokes, E.C., Unruh, G., Ürge-Vorsatz, D., 2016. Carbon lock-in: types, causes, and policy implications. Annu. Rev. Environ. Resour. 41, 425–452. https://doi.org/10.1146/annurev-environ-110615-085934.

Strunge, T., Naims, H., Ostovari, H., Olfe-Kräutlein, B., 2022. Priorities for supporting emission reduction technologies in the cement sector – a multi-criteria decision analysis of CO2 mineralisation. J. Clean. Prod. 340, 130712 https://doi.org/10.1016/j.jclepro.2022.130712.

Swiss Centre for Life Cycle Inventories, 2020. ecoinvent Data V 3.6.

Tanzer, S.E., Ramírez, A., 2019. When are negative emissions negative emissions? Energy Environ. Sci. 12, 1210–1218. https://doi.org/10.1039/C8EE03338B.

Tanzer, S.E., Blok, K., Ramírez, A., 2020. Can bioenergy with carbon capture and storage result in carbon negative steel? Int. J. Greenh. Gas Control 100, 103104. https://doi.org/10.1016/j.ijggc.2020.103104.

The National Academies Press, 2019. In: Negative Emissions Technologies and Reliable Sequestration: A Research Agenda. The National Academies Press, Washington, DC, p. 1 online resource (1.

Tiefenthaler, J., Braune, L., Bauer, C., Sacchi, R., Mazzotti, M., 2021. Technological demonstration and life cycle assessment of a negative emission value chain in the Swiss concrete sector. Front. Clim. 3, 729259 https://doi.org/10.3389/fclim.2021.729259.

Veetil, S.P., Hitch, M., 2020. Recent developments and challenges of aqueous mineral carbonation: a review. Int. J. Environ. Sci. Technol. https://doi.org/10.1007/s13762-020-02776-z.

Veld, H., Roskam, G.D., van Enk, R., 2009. Desk Study on the Feasibility of CO2 Sequestration by Mineral Carbonation of Olivine, p. 27. Netherlands. http://inis.iaea.org/search/search.aspx?orig_q=RN:40102549.

von der Assen, N., Jung, J., Bardow, A., 2013. Life-cycle assessment of carbon dioxide capture and utilization: avoiding the pitfalls. Energy Environ. Sci. 6, 2721–2734. https://doi.org/10.1039/C3EE41151F.

von der Assen, N., Müller, L.J., Steingrube, A., Voll, P., Bardow, A., 2016. Selecting CO2 sources for CO2 utilization by environmental-merit-order curves. Environ. Sci. Technol. 50, 1093–1101. https://doi.org/10.1021/acs.est.5b03474.

Wildbolz, C., 2007. Life Cycle Assessment of Selected Technologies for CO2 Transport and Sequestration.

Woodall, C.M., McQueen, N., Pilorgé, H., Wilcox, J., 2019. Utilization of mineral carbonation products: current state and potential. Greenhouse Gases: science and Technology. Greenhouse Gas Sci. Technol. 9, 1096–1113. https://doi.org/10.1002/GHG.1940.

World Steel Association, 2018a. LIFE CYCLE INVENTORY STUDY.

World Steel Association, 2018b. Production of Crude Steel in Electric Furnaces. https://www.worldsteel.org/steel-by-topic/statistics/steel-data-viewer/P1_crude_steel_EF/DEU/FRA.

Wuppertal Institute, 2018. Low-Carbon Infrastructure NRW: dekarbonisierungsstrategien und -technologien für energieintensive Industrien. Projektbericht. Wuppertal.

Zhang, S., Zhuang, Y., Tao, R., Liu, L., Zhang, L., Du, J., 2020. Multi-objective optimization for the deployment of carbon capture utilization and storage supply chain considering economic and environmental performance. J. Clean. Prod. 270, 122481 https://doi.org/10.1016/j.jclepro.2020.122481.

Zhou, C., Liu, P., Li, Z., 2014. A superstructure-based mixed-integer programming approach to optimal design of pipeline network for large-scale CO 2 transport. AIChE J. 60, 2442–2461. https://doi.org/10.1002/aic.14436.